*Review*

# Microneedles' Device: Design, Fabrication, and Applications

Cristiana Oliveira [1], José A. Teixeira [1,2] , Nelson Oliveira [3], Sónia Ferreira [3] and Cláudia M. Botelho [1,2,*]

1   CEB—Centre of Biological Engineering, University of Minho, Campus de Gualtar, 4710-057 Braga, Portugal; pg42888@alunos.uminho.pt (C.O.); jateixeira@deb.uminho.pt (J.A.T.)
2   LABBELS—Associate Laboratory, 4710-057 Braga/Guimarães, Portugal
3   BestHealth4U Lda, Praça Conde de Agrolongo, Edifício GNRation, Nº 123, 4700-312 Braga, Portugal; nelson.oliveira@besthealth4u.pt (N.O.); sonia.ferreira@besthealth4u.pt (S.F.)
*   Correspondence: claudiabotelho@ceb.uminho.pt

**Abstract:** The delivery of therapeutical molecules through the skin, particularly to its deeper layers, is impaired due to the stratum corneum layer, which acts as a barrier to foreign substances. Thus, for the past years, scientists have focused on the development of more efficient methods to deliver molecules to skin distinct layers. Microneedles, as a new class of biomedical devices, consist of an array of microscale needles. This particular biomedical device has been drawing attention due to its ability to breach the stratum corneum, forming micro-conduits to facilitate the passage of therapeutical molecules. The microneedle device has several advantages over conventional methods, such as better medication adherence, easiness, and painless self-administration. Moreover, it is possible to deliver the molecules swiftly or over time. Microneedles can vary in shape, size, and composition. The design process of a microneedle device must take into account several factors, like the location delivery, the material, and the manufacturing process. Microneedles have been used in a large number of fields from drug and vaccine application to cosmetics, therapy, diagnoses, tissue engineering, sample extraction, cancer research, and wound healing, among others.

**Keywords:** microneedles; bioactive molecules; transdermal drug delivery system; design parameters; manufacturing techniques; usage

## 1. Introduction

Skin is the largest organ in the human body. For several decades, it was only perceived as an "envelope" for the human body, aimed at separating the exterior from the interior. However, research has shown that the skin has multiple functions. Protection is one of them, but it is also involved in the immune system, thermal regulation, and even molecular synthesis [1]. Skin can be used as a gateway for medical applications, for example, transdermal drug delivery, where the molecules released can be systemically absorbed into the bloodstream [2–4].

While the skin can act as a gateway for the absorption of therapeutic molecules, its effectiveness is hindered by the numerous layers it possesses. In a sense, this process goes against the very purpose of skin. Therefore, several strategies have been developed over the years to overcome this resistance.

Treatments applied through the skin can be classified as invasive or non-invasive depending on whether the skin is pierced or not. Invasive therapy, such as blood glucose monitoring and intramuscular injections, are effective methods for providing information and delivering drugs, respectively [5]. However, there is a considerable likelihood of causing pain, allergies, and inflammation, limiting their applications. Non-invasive therapy can overcome the described drawbacks, but it is also limited by low accuracy, slowness, and ineffective controlled drug release [5].

In recent years, microneedle devices have garnered attention from the medical and scientific community due to their ability to breach the stratum corneum, forming micro-conduits that facilitate the passage of lipophilic and high-molecular-weight molecules [6].

A microneedle device is composed of an array of microneedles that can possess different properties depending on their application. For example, the length of microneedles is related to their specific function and intended application. They can range from 100 to 3000 μm, with the most common size varying from 250 to 1500 μm [7]. Through the formation of micron-level pores on the skin's surface, microneedles enable the penetration of macromolecular drugs into the stratum corneum in a minimally invasive manner, increasing penetration efficiency and facilitating the direct delivery of drug molecules to the dermis [8].

These devices not only allow the penetration of the stratum corneum but also aim to minimize contact with nerve endings and blood vessels as much as possible, thereby reducing pain during microneedle application [9–14]. Consequently, the transdermal local administration of microneedles provides patients with a convenient and painless method for self-medication [15], offering significant advantages over traditional intravenous administration. This is particularly beneficial for patients requiring long-term or even lifelong drug administration [16].

A microneedle device can also provide a rapid or long-term controlled release of drugs as a result of the rapid or slow degradation of the microneedle tip [17]. Figure 1 highlights both the benefits and the drawbacks of using microneedles [18].
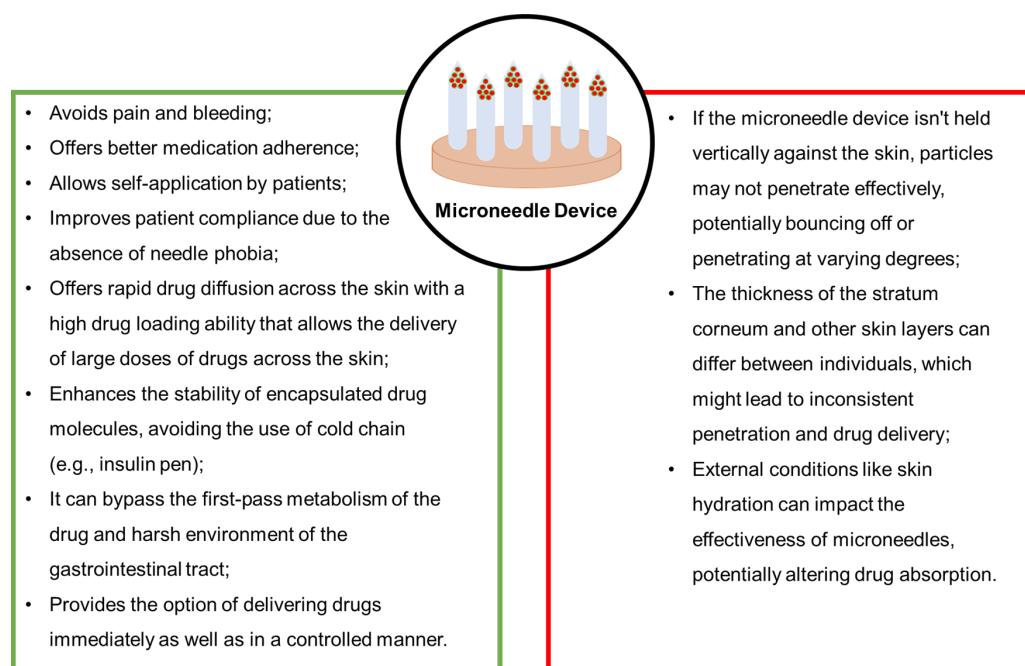


- Avoids pain and bleeding;
- Offers better medication adherence;
- Allows self-application by patients;
- Improves patient compliance due to the absence of needle phobia;
- Offers rapid drug diffusion across the skin with a high drug loading ability that allows the delivery of large doses of drugs across the skin;
- Enhances the stability of encapsulated drug molecules, avoiding the use of cold chain (e.g., insulin pen);
- It can bypass the first-pass metabolism of the drug and harsh environment of the gastrointestinal tract;
- Provides the option of delivering drugs immediately as well as in a controlled manner.

**Microneedle Device**

- If the microneedle device isn't held vertically against the skin, particles may not penetrate effectively, potentially bouncing off or penetrating at varying degrees;
- The thickness of the stratum corneum and other skin layers can differ between individuals, which might lead to inconsistent penetration and drug delivery;
- External conditions like skin hydration can impact the effectiveness of microneedles, potentially altering drug absorption.

**Figure 1.** The advantages (green) and limitations (red) of microneedle administration.

In addition to transdermal drug delivery, many emerging applications for microneedles have been revealed in recent years. These include an increased wound healing rate and tissue regeneration [19–21], treatment of dermatological diseases [22,23] and cancer [24], contraception [25], vaccine delivery [26,27], and diagnostic and monitoring health status [28,29].

In this review, we will firstly introduce different types of microneedles and discuss the most important characteristics that should be taken into consideration throughout the design process, such as needle length, tip diameter, and base width/diameter. Subsequently, we will describe various microneedles' fabrication methods and their applications.

## 2. Types of Microneedles

Microneedles can be composed by different materials and prepared by different methods, leading to microneedles with specific characteristics in terms of function and

morphology. According to the specific needs of the medical/cosmetic condition to be treated, a microneedle's structure can be categorized as solid, coated, dissolving, hollow, and hydrogel-forming.

All these distinct microneedle systems can be used to deliver substances, such as vaccines and biologic and small-molecule drugs. Each type of microneedle has its own way of delivering the drug into the target site [30]. Table 1 provides an overview of various delivery approaches and uses of microneedles.

**Table 1.** Delivery strategies and applications employed with distinct microneedle types.

| Type of Microneedles | Delivery Strategies | Applications | References |
|---|---|---|---|
| Solid | The poke-and-patch method involves the application of numerous microneedles to create pores as a preparatory step. Following this, a traditional drug formulation is applied to the skin surface. | Skin pre-treatment for the delivery of potassium chloride, insulin, vaccines, cosmetics, and antipsychotic medication; monitoring of glucose and lactate levels; urea sensing. | [31–37] |
| Coated | The coat-and-poke technique involves applying a water-soluble drug coating on solid microneedles. This coating dissolves during administration, depositing the drug directly into the skin. | Delivery of proteins, vaccines, parathyroid hormone, insulin, desmopressin, and dexamethasone; sampling, isolation, and identification of biomarkers; monitoring of glucose. | [38–45] |
| Dissolving | The poke-and-dissolve method utilizes biodegradable or water-soluble microneedles encapsulating drugs. These microneedles dissolve upon application, releasing their therapeutic payload into the skin. | Delivery of vitamin B12, vaccines, therapeutic peptides, adenosine, doxorubicin, triamcinolone acetonide, near-IR photosensitizer (Redaporfin™), genes, and sodium nitroprusside in combination with sodium thiosulfate, tofacitinib, flurbiprofen axetil, epidermal growth factor, and ascorbic acid. | [46–61] |
| Hollow | The poke-and-flow method involves microneedles with a hole in the center or side of their structure, allowing the drug to flow across the skin. | Delivery of teriflunomide, ceftriaxone sodium, mRNA, and vaccines; cell therapy; monitoring of glucose; synthetic amphetamine-type substance sensing; dermal interstitial fluid sampling and sensing. | [62–69] |
| Hydrogel-forming | The poke-and-release method utilizes water-insoluble microneedles injected into the skin, gradually releasing the encapsulated therapeutic molecule. The patch remains on the skin after application. | Delivery of albendazole, sildenafil citrate, metformin hydrochloride, methotrexate, and tuberculosis drugs; dermal interstitial fluid sampling. | [70–75] |

*2.1. Solid Microneedles*

The solid microneedle system was the first one developed and is mainly composed by metals like nickel, palladium, stainless steel, gold, and titanium; silicon; and polymers [18]. This type of microneedle is used for pre-treatment of skin. The needles are pressed into the skin, creating transitory micro-holes in the stratum corneum [76,77]. Subsequently, drugs are applied into the microporated skin in the form of a topical pharmaceutical formulation (gel, spray, ointment, cream, lotion, foam, or patch), facilitating the drug diffusion across the formed channels, leading the molecules to the target tissue (Figure 2) [78,79]. To fulfil the demands of painless and minimally invasive application, the microneedle strength applied into the skin must be low, but enough to pierce the skin. They require good mechanical properties and formability to guarantee that it does not break or buckle in use [17]. Given the ability to form fine incisions, solid microneedles can increase molecules' permeability up to four times [10]. Additionally, solid microneedles are easy to manufacture and can be utilized in the development of a coated microneedle system by applying drugs onto their surface. However, solid microneedles present some challenges. Firstly, they involve a

two-step application process, which can be inconvenient for patients. Secondly, micropores created by solid microneedles do not remain open for a long time due to the skin's natural healing capacity, potentially limiting the window for drug delivery [18]. On the other hand, due to an occlusive condition, micropores may remain open for up to 3 days [78], increasing the possibility of colonization by microorganisms under the patch, which can lead to a serious infection [80]. Since solid microneedles consist of sharp pieces made of non-biodegradable material, there is a risk of them remaining inside the skin upon the device removal [81]. Additionally, if highly viscous formulations need to be administrated, this system is not ideal, as the formulations may not flow smoothly into the formed pores, resulting in a lack of precise control over the dosage [78]. In summary, this system has residuals of sharp solid waste, poor biocompatibility, and an uncontrollable drug dose, thus limiting its application in tissue regeneration [80,82].
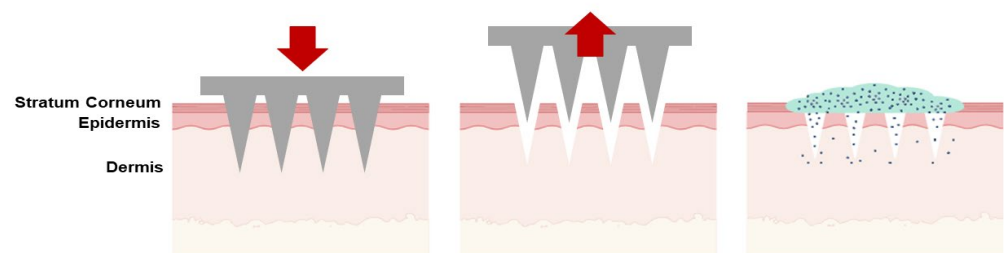


**Figure 2.** Drug delivery process using solid microneedles. Red arrows indicate the movements direction.

### 2.2. Coated Microneedles

The manufacture of coated microneedles involves the preparation of either solid or hydrogel microneedles, followed by their coating with a drug solution or dispersion [83]. Upon the insertion of the coated microneedle system into the skin, the coated drug is released (Figure 3) [15]. Typically, the coating dissolves within a few minutes of application, after which the naked microneedles are removed from the skin [84]. The solid film used as a coating generally comprises active compounds and water-soluble inactive excipients. These excipients dissolve in the interstitial fluid, causing the coating to detach from the microneedle surfaces [17]. Various active compounds, such as small molecules, peptides, proteins, short nucleic acids, DNA, viruses, virus-like particles, polymer particles, and insoluble inorganic particles, have already been coated onto microneedles [85–87]. Coated microneedles offer a single-stage application that does not require a drug reservoir [18]. However, the drug loading capacity is limited to a maximum of 1 mg [88], with the amount of drug loaded depending on the coating method, microneedle size, and coating layer thickness [89].
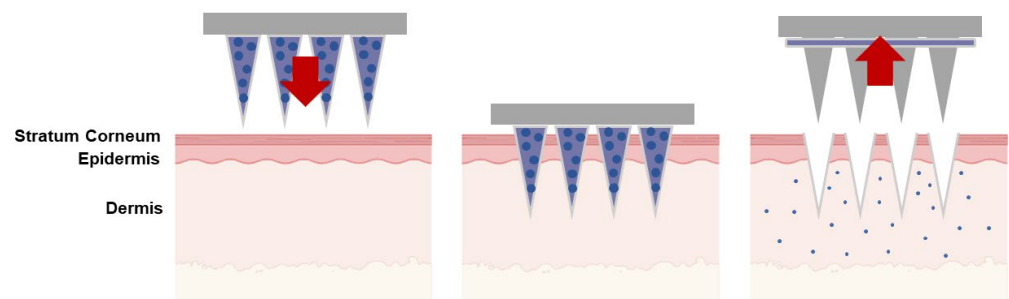


**Figure 3.** Drug delivery process using coated microneedles. Red arrows indicate the movements direction.

### 2.3. Dissolving Microneedles

Dissolving microneedles are typically prepared from water-soluble sugars such as trehalose or raffinose. They can also be prepared using biodegradable polymers like polyvinyl

pyrrolidone (PVP) and polyvinyl alcohol (PVA) [18]. A common fabrication technique for these microneedles is the solution-cast micromolding method, which utilizes a cavity prepared from polydimethylsiloxane (PDMS) as a master mold [90]. This type of microneedle can disperse or encapsulate the drug within the needle body [17]. During administration, the dissolving microneedles are inserted into the skin and completely dissolve upon contact with interstitial fluid, leading to the local release of the drug (Figure 4) [17,18].
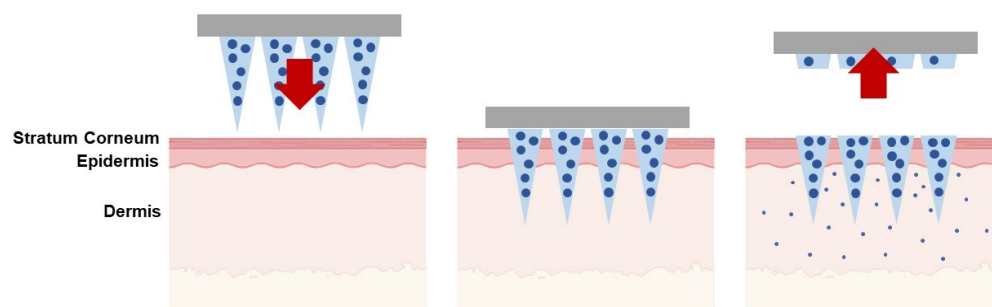


**Figure 4.** Drug delivery process using dissolving microneedles. Red arrows indicate the movements direction.

Contrary to the above-mentioned microneedle types, dissolving microneedles do not require a removal step, making them more patient-friendly. These microneedles reduce the likelihood of needle-stick injuries and leave no bio-contaminated residue within the skin [18]. Additionally, the delivery dose can be precise because the microneedles completely dissolve within the skin, eliminating the risk of drug loss during delivery or encapsulation [78].

Dissolving microneedles offer the advantages of a simple manufacturing process, a wide variety of materials for preparation, a low risk of cross-infection, and an absence of sharp waste residue [17]. They can be employed in long-term therapies with controlled release using biodegradable polymers such as polylactic acid (PLA) and poly(lactide-co-glycolic acid) (PLGA) [91]. Dissolving microneedles also boast a higher drug loading capacity (up to 33 mg) compared to coated microneedles [92].

However, dissolving microneedles may have inferior mechanical strength, resulting in a lower ability to penetrate the skin. This issue can be exacerbated by the use of sugars in the manufacturing process due to their hygroscopic nature [18]. Indeed, the properties of dissolving microneedles, such as mechanical strength, the dissolution rate, and tissue penetration, depend on the material used in their fabrication [93]. For example, hyaluronic acid (HA) microneedles exhibit a faster dissolution rate, better mechanical strength, and less shrinkage than microneedles prepared with carboxymethyl cellulose (CMC), gelatin, and sodium alginate (SA) [94]. Furthermore, microneedles prepared with synthetic polymers such as PLGA and PLA typically have suitable mechanical properties combined with a slow degradation rate [94]. The materials commonly used for the manufacture of dissolving microneedles and their advantages and disadvantages are described in Table 2.

**Table 2.** Advantages and disadvantages of the materials commonly used for the manufacture of dissolving microneedles.

| Materials | Advantages | Limitations | References |
|---|---|---|---|
| Maltose | Biocompatible; No dermatological issues were noted on the human skin following insertion; High mechanical strength; Easy degradation; Fast dissolution; Controllable viscosity; Drug stability enhancer; Efficiently deliver protein drugs; Accelerate drug delivery. | High melting point is unfavorable for heat-sensitive drugs; The use of microneedles in a humid environment is limited due to the poor moisture resistance. | [95–98] |
| Hyaluronic acid (HA) | FDA-approved; Biocompatible; Biodegradable; Water solubility; Faster rate of dissolving; Enhance mechanical strength of dissolving microneedles; Quickly release drugs; Nontoxic and non-irritant; HA can be utilized for extended durations; No hypersensitivity effects or side effects associated with HA microneedles were identified in clinical studies. | Poor moisture resistance; Easy to shrink after microneedle fabrication. | [51,99–103] |
| 2-Hydroxypropyl-β-cyclodextrin (HP-β-CD) | Improve the solubility of poorly water-soluble drugs by forming inclusion compounds; Enhance mechanical strength of dissolving microneedles. | Selective inclusion. | [51,99,104] |
| Carboxymethylcellulose (CMC) | FDA-approved; Biocompatible; Biodegradable; Dissolve quickly in water; Can achieve slow and controllable release of drugs; In vitro cytotoxicity analysis and in vivo tissue response test did not show any side effects after treatment with CMC microneedles. | Poor moisture resistance; Poor mechanical strength. | [91,105,106] |
| Chitosan | Biocompatible, biodegradable, and nontoxic; It can either be cleared by the kidneys in vivo or degraded into fragments that are subsequently cleared by the kidneys; Antibacterial properties; Sufficient mechanical strength to penetrate porcine cadaver skin; Strong adsorption ability. | Limited raw materials; Negative water solubility. | [107–111] |
| Starch | Non-cytotoxic; Biodegradable; Higher mechanical strength than CMC. | Pure starch is more rigid and prone to fracturing and exhibits inferior film-forming characteristics. | [112–114] |
| Gelatin | Excellent biodegradability, biocompatibility, film formation, gelation, emulsification, water retention, and drug loading ability; Provides high safety and slow release. | Toughness of gelatin is poor, and it is easy to fracture; Low melting point and poor stability. | [107,112] |
| Silk fibroin | FDA-approved biomaterial; Non-cytotoxic, biocompatible, and the in vivo degradation products are non-inflammatory; Adequate mechanical force to pierce mouse skin for drug delivery; High tensile strength and toughness; Excellent mechanical characteristics, efficient gradual release of drugs, and favorable processing conditions. | Long fabrication time. | [115–120] |
| Poly(vinylpyrrolidone)(PVP) | Sufficient strength to pierce mouse skin; Enables the avoidance of organic solvents and high temperatures, aiding in the preservation of the drug's stability and efficacy; Biocompatible and biodegradable; Low oral and transdermal toxicity; Non-irritating to skin; No adverse effects related to treatment were observed in a 6-month study. | Poor moisture resistance. | [112,121–125] |

**Table 2.** *Cont.*

| Materials | Advantages | Limitations | References |
|---|---|---|---|
| Polyvinyl alcohol (PVA) | Sufficient strength to penetrate both porcine cadaver skin and mouse skin; FDA-approved material; Biocompatible; Biodegradable; Good viscosity and toughness; Low cytotoxicity; Dissolve quickly in water. | Poor moisture resistance. | [107,126–128] |
| Polylactic acid (PLA) | FDA-approved biomaterial for the use of implants in humans; Biocompatible; Biodegradable; The in vivo degradation products are nontoxic; Excellent mechanical strength; High modulus of elasticity. | Fabrication of microneedles typically necessitates high temperatures (exceeding 170 °C) or organic solvents. | [31,107,129] |
| Polyglycolic acid (PGA) | FDA-approved biomaterial; Biocompatible; Biodegradable; The in vivo degradation products are nontoxic; Excellent mechanical strength to penetrate the regenerated human skin. | Fabrication of microneedles typically necessitates high temperatures or organic solvents. | [130] |
| Poly(lactide-co-glycolic acid) (PLGA) | Outstanding mechanical strength to pierce the murine skin; FDA-approved biomaterial; Biocompatible; Biodegradable; The in vivo degradation products are nontoxic. | Fabrication of microneedles typically necessitates high temperatures or organic solvents. | [129,131,132] |
| Polycaprolactone (PCL) | FDA-approved biomaterial; Biocompatible; Biodegradable; Non-cytotoxic; The in vivo degradation products are nontoxic; Sufficient mechanical strength to penetrate porcine cadaver skin for drug delivery. | The processing temperature is comparatively lower than PLA, PGA, and PLGA, yet still above 50 °C, which poses a constraint on incorporating heat-sensitive drugs such as insulin. | [129,133] |

### 2.4. Hollow Microneedles

Hollow microneedles feature a central or side lumen, with diameters ranging from 5 to 70 μm. They can be filled with a drug solution or dispersion or remain hollow and connected to a drug reservoir [18]. These microneedles create a pathway for the drug to flow directly into the epidermis or the upper layer of the dermis after insertion into the skin (Figure 5) [134]. Hollow microneedles can be fabricated from various materials, including metal, silicon, and polymers [17]. Their primary advantages include precise control over the amount of drug release and the drug release rate [6]. This type of microneedle is well suited for delivering biological macromolecular drugs and a higher dose of molecules [10,16]. Hollow microneedles represent an effective strategy for administering traditional injectable preparations, thus expanding their application spectrum to include fluid drug micro-injection and minimally invasive tissue/blood extraction [135]. However, hollow microneedles have some limitations, such as the risk of a needle blockage or even blowout. Additionally, their complex fabrication process poses a challenge [93,136,137].
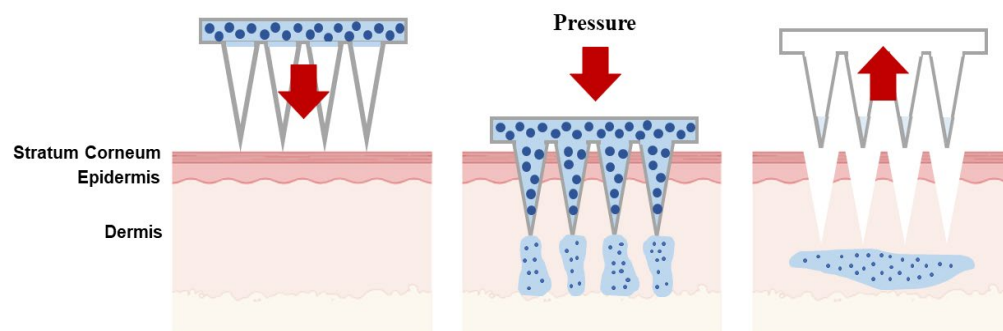


**Figure 5.** Drug delivery process using hollow microneedles. Red arrows indicate the movements direction.

## 2.5. Hydrogel-Forming Microneedles

Hydrogel-forming microneedles are integrated systems composed of two parts: an array of microneedles formed by a crosslinked polymer and a drug reservoir at the back, which can take various forms such as films, patches, lyophilized, and compressed tablets [18]. The polymer used must be a hydrocolloid, such as cellulosic derivatives, capable of absorbing a substantial volume of interstitial fluid into their 3D structure and swelling upon insertion into the skin [138,139]. Upon insertion, the microneedles draw up interstitial fluid, forming a swollen polymeric matrix with numerous capillaries inside. This process creates continuous microchannels connecting the drug reservoir to the capillaries, thereby enhancing the delivery of drugs into the surrounding tissue (Figure 6). The swollen polymeric matrix acts as a membrane for controlling the rate of release. After the drug release is complete, the empty polymeric needles are removed from the skin [18]. This type of microneedle offers more flexibility in terms of shape and size. The ability to remove the empty microneedles from the skin without leaving any polymeric residue is highly beneficial. Additionally, due to microneedle composition, it is possible to modulate the density of the hydrogel matrix to achieve a specific drug delivery rate [18]. Hydrogel-forming microneedles can accommodate a reasonable drug loading, but they may exhibit poor mechanical strength and physical stability [140].
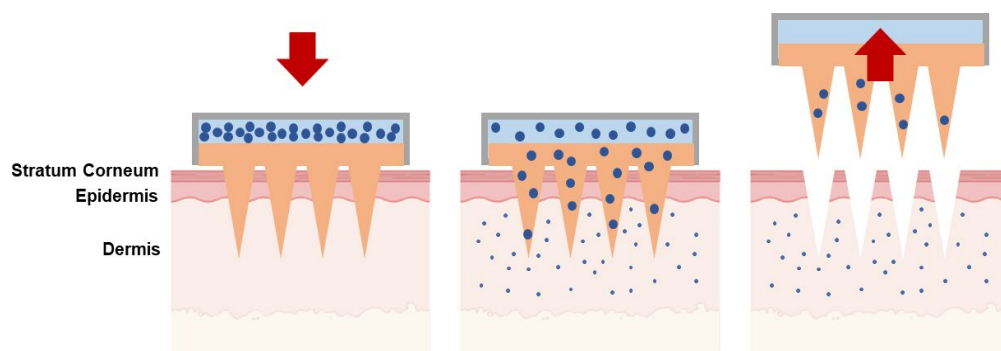


**Figure 6.** Drug delivery process using hydrogel-forming microneedles. Red arrows indicate the movements direction.

## 3. Microneedle Design

While designing microneedle systems, it is essential to meticulously plan various parameters as they play a crucial role in facilitating drug delivery to the intended target site [141].

### 3.1. Length

In a transdermal application it is necessary to take into consideration that human skin contains three layers, each with different thicknesses—the stratum corneum (10–20 μm thick) [142,143], epidermis (100–150 μm thick) [144], and dermis (3–5 mm thick) [145,146]. To evaluate the ability of a microneedle system to pierce skin, Verbaan et al. tested a microneedle system with a constant base diameter, 300 μm, and distinct needle lengths (300, 550, 700, and 900 μm). The study demonstrated that microneedles with a length of 300 μm could not penetrate human skin, while microneedles with a length above 550 μm successfully pierced skin [145]. These results suggest that the microneedles required an optimum length to penetrate skin smoothly. Similarly, Donnelly et al. showed that an increase in microneedle length led to a meaningful increase in penetration depth [146]. However, it is necessary to take into consideration that longer needles may lead to molecule release into the lower end of the dermis and their absorption by skin microcirculation [147,148]. It is also important to bear in mind that nerve endings are distributed in the deep dermis of the skin, so a microneedle with a longer length is more likely to activate pain receptors, or puncture capillaries, causing bleeding, which may reduce patient acceptability [149].

Gill et al. studied the correlation between microneedle length and pain. The authors demonstrated that an increase in the microneedle length from 480 μm to 1450 μm resulted in more than a seven-fold increase in pain (from 5% to 37% in participants) [150].

### 3.2. Needle-to-Needle Spacing

Taking into consideration the relationship between needle length and pain, distinct strategies can be employed to increase penetration depth, such as a higher force of application or a larger needle-to-needle spacing [9,146,151]. Donnelly et al. verified that a microneedle array with a 600 μm height penetrated neonatal porcine skin to a depth of 330 μm with an insertion force of 4.4 N/array, while an insertion force of 16.4 N/array led to a significant increase in the penetration depth, 520 μm under [146]. On the other hand, Kochhar et al. showed that an increase in needle spacing (varying between 2× and 6× base diameter) leads to an increased force of application per needle, resulting in higher skin (from rat abdomen) penetration depth [151]. A study using neonatal porcine skin showed that the required insertion force for a successful tissue penetration decreased from 0.030 to 0.028 N per needle as the needle-to-needle spacing increased from 30 to 150 μm. However, this correlation between insertion force and needle-to-needle spacing was weaker if the needle-to-needle spacing was higher than 150 μm [152].

### 3.3. Tip Diameter and Tip Angle

To avoid a microneedle's fracture while piercing the skin, microneedle design should take into account the tip radius, angle, and length/base diameter ratio [153,154]. The microneedles' tip diameter influences the contact area between the microneedle and the skin, and consequently the insertion force. In this way, smaller areas result in smaller insertion force, which in turn leads to a smaller skin deformation and thus a greater chance of penetration [151,154–156]. Römgens et al. monitored the penetration force and depth of single solid microneedles and concluded that the smaller the needle tip diameter (5 μm), the smoother the penetration. On the other hand, with a larger tip diameter, the penetration of the system in human ex vivo skin was more abrupt. They also concluded that a tip diameter smaller than 15 μm is fundamental for inserting microneedles into the desired depth of skin in a well-controlled manner [157]. A similar study revealed a decrease in the force required to pierce the stratum corneum from 3.04 to 0.08 N per needle, when the tip radius was reduced from 80 to 30 μm. In fact, microneedle penetration was improved due to a greater pressure at the tip created by the smaller contact area between the microneedle and the skin [158].

The tip angle is another important parameter that influences skin penetration. Bao et al. suggested that a tip angle of 30° can easily pierce the skin [159]. Sabri et al. also verified that biodegradable microneedles with low tip angles (15–30°) and thin needle shafts of 120 μm effectively improved microneedle insertion without causing tensile failure [158].

### 3.4. Aspect Ratio

The base diameter and length of microneedles are normally considered together. In fact, the microneedles' sharpness is expressed by the aspect ratio, i.e., the ratio of the length of the microneedle to its diameter of the bottom [149]. The aspect ratios of microneedles directly affect their mechanical properties. Indeed, microneedles possessing a higher aspect ratio exhibit a reduced base area, thereby resulting in lower yield force or fracture force [160]. This circumstance could potentially cause microneedle breakage during application, resulting in failure to deliver the drug to the intended target site [155,161].

Kochhar et al. [151] examined the impact of needle tip spacing, base diameter, and length on skin penetration. They found that a length of 827 μm and a base diameter of 200 μm resulted in a slower penetration rate compared to a base diameter of 300 μm and a length of 400 μm. The researchers suggest that a greater aspect ratio correlates with inferior mechanical properties of both the needle tip and body. Bending takes place prior to reaching the insertion force during the piercing process, leading to a reduced penetration

rate and consequently, a lower piercing rate. Another paper confirmed this theory [162]. Gittard et al. fabricated polymer microneedles with varying aspect ratios and assessed the average stiffness of these microneedles through compression testing [162]. The results revealed that the stiffness of polymer microneedles with aspect ratios of 2, 2.5, and 3 are 7580 N/m, 2222 N/m, and 1620 N/m, respectively. In this way, it can be concluded that the resilience of polymer microneedles against deformation declines with an increase in the aspect ratio. Specifically, when comparing microneedles of the same length, those with a larger base diameter exhibit superior mechanical properties.

*3.5. Needle Geometry*

The needle geometry also considerably affects the penetration of the microneedles in the skin, being a determinant factor in drug loading, stress distribution, and mechanical properties [94]. Li et al. engineered dextran-based microneedles loaded with ovalbumin, featuring various geometries including cone, cone-cylinder, rectangular pyramid, and hexagonal pyramid shapes [163]. In the study, it was demonstrated that the cone was more advantageous in drug loading capacity than the other designs since it was the one with the highest volume ratio. Moreover, the highest penetration was achieved by cone microneedles, and the lowest was by cone-cylinder microneedles. Indeed, the skin insertion ratios were 97.8%, 76.2%, 49.6%, and 38.8% for the cone, rectangular pyramid, hexagonal pyramid, and cone-cylinder geometries, respectively [163]. Loizidou et al. concluded that triangular and square-based microneedles have a greater penetration depth than hexagonal-based microneedles at a constant microneedle length and spacing, which is attributed to the fact that hexagonal-based microneedles start penetrating the stratum corneum less easily [164].

## 4. Microneedle Fabrication Methods

There exist numerous techniques for fabricating microneedles. This section outlines the predominant methods employed not just for crafting microneedles themselves, but also for producing molds tailored to microneedle fabrication. Indeed, microneedles can be manufactured either directly or via a mold, particularly when aiming for cost-effective large-scale production. Table 3 summarizes the pros and cons of various methods discussed in this section.

**Table 3.** Advantages and limitations of various microneedle fabrication techniques.

| Fabrication Method | Advantages | Limitations | References |
|---|---|---|---|
| MEMS-based methods | Very precise geometries; Smooth vertical sidewall. | Time consuming; Expensive; Difficult to fabricate complex structures; Basic material limited to silicone and photocurable polymers. | [165,166] |
| Micromolding | High precision; Cost effective; Used for mass production; A large variety of basic material. | Difficult to fabricate complex structures; Drug load capacity; Mechanical behavior; Controls the depth of penetration. | [165,166] |
| Laser ablation | Less time consuming. | Might cause a crack or fatigue resistance on the substrate (microneedle array); Expensive; Not suitable for large fabrication. | [166] |
| Injection molding | Mass production; Cost effective. | High initial cost (machine equipment cost); Complex process. | [166] |

*4.1. Microelectromechanical Systems (MEMSs)*

MEMS methods can be used to manufacture hollow and solid microneedles, as well as molds for dissolving microneedles, directly from an appropriate material substrate (like

silicon wafer) [15]. The fabrication process for microneedles, along with molds using this technique, involves a meticulously controlled three-step process—deposition, patterning, and etching of materials [167,168]. In this way, complex three-dimensional structures emerge as a result of variations in etchant selectivity among different materials [168].

The first step consists of forming a film with a thickness ranging from a few nanometers to 100 μm on a substrate through chemical or physical vapor deposition [167,169,170]. In this way, the film can be formed through the chemical reaction on the substrate surface (chemical vapor deposition process) or by atoms transferred directly from the source to the substrate through the gas phase (physical vapor deposition process) [168,170].

Subsequently, during the second stage of the process, named patterning, a two-dimensional master pattern of the desired material is transferred from the initial photomask to the substrate coated with photosensitive material. Typically, a silicon wafer serves as the substrate, and the transfer process is conducted using a radiation source in one of the lithography techniques (photolithography [171], ion beam lithography, or X-ray lithography [172]) [168,173]. The most common type of lithography used is photolithography, which is activated by ultraviolet light and an X-ray onto diverse photosensitive polymers, including SU-8 [174], poly (methyl methacrylate) (PMMA) [175], KMPR® [176], polyethylene glycol diacrylate (PEGDA) [177], and chitosan lactate [178]. This process also enables the manufacture of molds for microneedles. In this scenario, a rigid silicone mold with a positive image is initially created, and subsequently, a negative mold is produced from PDMS. Then, the desired material is applied [170]. Photolithography can be very advantageous, since its selective shape-forming property allows the production of microneedles based on photosensitive polymers without the help of etching [174,175,177]. Nevertheless, for the fabrication of silicon-based microneedles, etching is necessary. This process typically follows lithography and involves removing the non-masked but unwanted parts on the silicon substrate, as is common in traditional MEMS fabrication [165].

During the third stage of the process, referred to as etching, a potent acid or caustic agent is applied to dissolve the exposed areas of the substrate, shaping the material on the substrate into the desired design [168]. Two major types of the etching process are wet etching and dry etching [179], the first one being used to polish and sharpen the structures, while the last one is utilized to drill holes in hollow microneedles made of metals, as well as to control the height of the needles [180–182]. In the wet etching process used to produce arrays of metallic or silicon microneedles, surplus material is eliminated by immersing the substrate in a chemical liquid. Etching can be carried out at uniform rates (isotropic etching) or varying rates (anisotropic etching) [167,183]. In turn, the dry etching process consists of using a vapor phase or plasma etcher. Two major types of dry etching are recognized—reactive ion etching and ion-beam milling [79,168]. In reactive ion etching, the gas is excited into a reactive state, facilitating a reaction between the gas and the substrate. The gas pressure is controlled to adjust the number of ions that affect the degree of isotropy. The electric field can accelerate ions, thus enhancing the direction of etching. Concerning the ion-beam milling process, inert ions are sped up from a source to physically remove the material to be etched [79,168]. Even though reactive ion etching creates structures, it often suffers from a low etching rate, and maintaining a high width-to-height ratio can be challenging. Deep reactive ion etching, frequently called the Bosh process, is suitable for the fabrication of off-plane microneedles, and it can be used to manufacture hollow microneedles with a lumen of several hundred micrometers (width-to-height ratio of 30:1) [184]. Wet etching generally lowers fabrication expenses compared to dry etching. However, the optimal outcomes are typically attained through a combination of isotropic dry and anisotropic wet etching, resulting in well-defined and sharp microneedle tips [15,184,185].

Numerous studies in the literature showcase the efficacy of MEMS techniques in manufacturing both microneedles and molds. For example, the deep reactive ion etching process was used by Henry et al. to manufacture silicone, out-of-plane microneedles. In this case, the chromium masking material was initially deposited onto a silicon wafer and

shaped into dots with a diameter matching the base of the intended microneedles. After-wards, with the aim of preserving the regions protected by the metal mask and allowing the microneedles to form, the wafers are exposed to reactive ion etching [186]. Furthermore, Wang et al. demonstrated the development of hollow microneedles through a two-stage production process—primarily, they fabricated a PDMS mold using photolithography to reach the pyramidal top profile; then, they made hollow SU-8 microneedles on a built-in PDMS mold [187]. They also achieved an increase in encapsulation in the micro-trenches by decreasing its viscosity. They also achieved an increase in encapsulation in the micro-trenches by heating the microneedles to 60°C and consequently reducing its viscosity [187]. Paik et al. developed an in-plane array of single crystal silicon microneedles integrated with a PDMS microfluidic chip for blood extraction in point-of-care devices and drug delivery systems [188]. The production method of these microneedles included anisotropic dry etching, isotropic dry etching, and the trench-refilling process. The researchers demon-strated that the developed microneedles were sufficiently rigid to penetrate animal skin models without causing damage [188]. Additionally, hollow microneedles were developed on the silicon substrate using inductively coupled plasma and anisotropic wet etching techniques [189]. Afterwards, these microneedles were integrated with the PTZ pump for a precise insulin dosage. Ultimately, Ma et al. concluded that the developed system can be used for programmable drug delivery or fluid sampling [189]. Wang et al. de-scribed three methods for producing microneedle arrays based on MEMS technology—the planar pattern-to-cross-section technology (PCT) method using LIGA (Photolithography, Galvanogormung, Abformung) technology to obtain a three-dimensional structure similar to an X-ray mask pattern; silicon wet etching combined with the SU-8 process to obtain a PDMS quadrangular pyramid microneedle array using PDMS transfer technology; and the tilting rotary lithography process to obtain a PDMS conical microneedle array on an SU-8 photoresist through PDMS transfer technology [190]. The researchers demonstrated that these three methods can produce microneedle arrays with a high aspect ratio and sharp tips, which provides a good guarantee for microneedle arrays to penetrate the skin. In the case of the PCT technology, the cost is high and the process is complex [190]. Regarding the engraving process and the tilting rotary exposure process, they are simple to operate, and the developed microneedle array mold has good repeatability and accuracy. Afterwards, PDMS microneedle array molds can be achieved by employing the PDMS transfer technol-ogy. The use of these molds allows the preparation of a drug-loaded microneedle array of dissolved materials [190].

In short, MEMS-based methods are able to manufacture photosensitive-polymer-based and silicon-based microneedles [165]. Indeed, the described methods enable the production of common structures, such as conical, pyramid-like, and hollow needles, with high precision. Another benefit of MEMS-based methods is the possibility of changing the needle length and tip angle by simply tuning parameters. However, these methods also have some disadvantages like the fact that the entire process is expensive and time-consuming. Moreover, microneedles with complex structures, such as core–shell, stacked, and adhesive structures, cannot be manufactured by these methods [165].

### 4.2. Micromolding

Micromolding currently stands as the predominant technique for manufacturing mi-croneedles. Essentially, this process involves utilizing a negative mold with cavities for needle formation and material loading. Once the material is filled and cured, a complete mi-croneedle can be extracted from the negative mold [165]. This technique is suitable for vari-ous materials including natural and synthetic polymers, ceramics, hydrogels, etc. [191,192]. To accommodate different material properties, various curing or shape-forming methods such as solvent evaporation, photo-crosslinking, chemical crosslinking, melt solidification, sintering, freezing, and freeze–thawing are also employed [193–197]. Moreover, the produc-tion of biodegradable polymer microneedles has been reported, comprising both natural

and synthetic materials, featuring appropriate geometry and ample strength to penetrate the skin [153,198].

Micromolding can be very advantageous since it is a simple, inexpensive, and highly reproducible technique [165]. Furthermore, a composite microneedle can be readily created by sequentially adding distinct materials and cargos into the same mold. Taking this into account, different structures, such as multiregional, core–shell, stacked, swelling, and suction cup structures, can all be produced by this process, which have complex release kinetics and functions [165].

However, micromolding also has issues in terms of mold-filling. In fact, surface tension plays a significant role at the microscale, posing a challenge for materials to fill into the mold cavity against the force of gravity. Therefore, investigators have developed various mold-filling techniques to counter surface tension, including vacuum [196], centrifugation, imprinting [199,200], spinning coating [201], atomized spray, and infiltration [202,203]. Other limitations of the method described include its inability to form complex structures, such as adhesive structures with barbs and a hollow structure, as well as the possibility of damaging the final structures due to demolding stress, in the case of soft and fragile materials like hydrogels. The challenges of controlling the depth of penetration, the load capacity of the drug, and the mechanical behavior of the polymer are also some of the drawbacks of the micromolding process [204]. Additionally, this technique is not suitable for processing materials such as metal, silicon, and glass [165].

### 4.3. Laser Cutting

Microneedles, specifically metal microneedles, can be fabricated by 3D laser cutting [82,150,205–208], laser ablation [209–211], and electroplating or electroless plating of metal onto positive or negative microneedle molds [15].

Arrays of solid microneedles can be manufactured by cutting stainless steel or titanium sheets in the form of microneedles with an infrared laser [168]. Moreover, the computer-aided design (CAD) software is normally used to create the desired characteristics of microneedles, such as shape, geometry, and dimensions. In this way, the laser beam follows the predefined shape of the needle; afterwards, microneedles are cleaned in hot water and bent at 90 degrees, vertically from the plane of the base [168]. Subsequently, the prepared microneedles are electropolished, washed, and dried with compressed air in order to deburr, reduce the thickness of microneedles, and sharpen the tips [168]. This technique is useful since it allows us to produce a single row of microneedles of different geometries, as well as two-dimensional rows of metallic microneedles [82,150,205–208].

Additionally, this method has been used in the manufacture of hollow microneedles [212] and molds for a dissolving microneedle patch [213]. In the production of hollow microneedles, holes were created on the side of PLA sheets using a KrF laser ($\lambda$ = 248 nm). These sheets had been previously manufactured using a micromolding technique [212]. On the other hand, Albarahmieh et al. described the production of microneedle patches by employing a $CO_2$ laser on polymethylmethacrylate (PMMA) sheets. Afterwards, a specific mixture was poured into PMMA molds, resulting in the creation of dissolvable microneedles containing methylhydroxy-4-benzoate and terbinafine hydrochloride [213].

The utilization of a $CO_2$ laser cutter for the development of microneedle master molds has several advantages, such as the fact that it is a cleanroom-free and low-cost fabrication method, and it allows a rapid manufacture of microstructures when compared to the conventional time-consuming photolithography process [214]. Furthermore, this technique is accessible for the batch production of microneedle patches with the benefit that the geometry can be modified at any time [215]. The fabrication process consists of loading the two-dimensional geometric design into the system to create the desired shape in the substrate. It is an overall two-stage efficient process used to produce distinct geometries and dimensions of a solid microneedle height less than 2.5 mm [216]. Anbazhagan et al. used a $CO_2$ laser and polymer molding technique to produce a 10x10 designed microneedle array structure [217]. In the study, it was revealed that the laser engraving method could

directly create different geometries of microneedle molds by varying the laser scan speed and power. Moreover, microneedles were manufactured by casting the PDMS on the acrylic mold (produced by $CO_2$ laser) and these microneedles showed high mechanical strength for good skin penetration [217].

### 4.4. Laser Ablation

Laser ablation, also known as photoablation, is a process involving the removal of material from a solid (or sometimes liquid) surface by irradiating it with a laser beam. Typically, this method involves using a pulsed laser to remove material, although it is feasible to ablate material with a continuous wave laser beam if the laser intensity is sufficiently high [134]. Lasers are widely used to process distinct materials ranging from the microscale to nanoscale for various applications [218–226]. Several laser types have been explored for the fabrication of microneedle arrays, including $CO_2$ [214,227], UV excimer [212,228], and femtosecond laser machines [229].

Laser ablation can be used to shape any metal and it is an effective and fast method for microneedle production. Indeed, the laser beam requires 10 to 100 nanoseconds to reach the threshold point on the material sheet [166]. Furthermore, this technique is linked with thermal effects at the cutting surface, causing alterations in the microneedle structure and mechanical properties. These changes could potentially lead to undesired outcomes such as cracking or reduced fatigue resistance in the microneedles [230,231]. The laser ablation technique is a non-contact process that imposes low heat loads on the substrate [166]. On the other hand, the cost of laser equipment is higher compared to other types of machinery, and the method described is not well suited for large-scale production [230].

A team of researchers presented a pioneering and efficient method for producing metal microneedles, utilizing circularly polarized optical vortices with non-zero total angular momentum. They showcased the fabrication of a tantalum microneedle array with a vertical height exceeding 10 μm and remarkably small tip radii [210]. Additionally, Evens et al. reported a novel technique for the manufacture of solid polymer microneedles using laser-ablated molds [211]. Molds are also applied in the injection molding process for the fabrication of polymer microneedles. Therefore, the height of microneedles can be altered, and a sharp tip radius can be achieved using this low-cost fabrication method [211].

In the case of dissolving microneedles, they can be fabricated using a two-step process, which begins with the production of a mold and then the fabrication of microneedles by using a casting process that involves vacuum molding [232,233]. The molds can be manufactured by employing a laser engraving machine to emit a laser beam to drill on the surface of PDMS sheets and create micro-cavities. This method allows the control of the microstructures of molds by laser power, speed, and imported patterns in the laser engraving machine [232,233]. Furthermore, microneedles fabricated using these molds revealed good capabilities of penetrating the stratum corneum of skin and delivering drugs to subcutaneous tissues. In short, the method described has several advantages, such as the fact that it is a simple direct manufacture method with the possibility of controlling the microstructures and can be used for large-scale production [232].

### 4.5. Drawing-Based Methods

Drawing-based methods encompass a range of techniques utilizing various drawing forces such as mechanical force, adhesive force, electrostatic force, and centrifugal force on precursor materials to form microneedle-like shapes. Subsequently, a specific curing process is employed for microneedle production [165].

Mechanical force drawing originated from the traditional drawn glass micropipette techniques [234]; therefore, it can only manufacture hollow glass microneedles. Indeed, the following has been reported: the fabrication of glass microneedles by pulling fire-polished borosilicate glass pipettes exposed at a high temperature with a micropipette puller and beveler [235,236]. In the first study, the developed microneedles provided an effective delivery of bolus insulin to patients diagnosed with type 1 diabetes [235]. In relation to the

other study, it was proven that glass microneedles could infuse milliliters of fluid into the skin [236]. Additionally, Mahadevan et al. manufactured microneedles using this method and demonstrated the successful delivery of 6-aminoquinolone and Rose Bengal to the eye, allowing intraocular drug delivery in a less invasive and less painful way than macroscale hypodermic needles [237].

Contact drawing methods primarily rely on the adhesive force between the material and the drawing device to produce microneedle structures. This is followed by specific shape-forming processes such as solidification, solvent evaporation, and ionic crosslinking [95,238,239]. The droplet-born air blowing method, proposed by Kim et al., is an example of a contact drawing method [238]. This method consists of using air blowing to shape polymer droplets into microneedles, allowing production under mild conditions, without the use of UV radiation or heat [168,198]. The first step of the process involves the dispersion of the prepared solution onto two plates (upper and lower), followed by positioning the upper plate downwards to allow contact between the droplets. As the upper plate moves upward, it stretches the viscous solution. Afterwards, blowing air removes any remaining water and solidifies the droplets into the desired shape by detaching them from the substrate [55,238,240,241]. This technique also allows precise control over the size of drops and the concentration of API by applying one drop of polymer per microneedle. Another advantage of the described process is its short duration. Moreover, it was utilized to produce dissolving microneedles loaded with insulin, which effectively reduced blood glucose levels in diabetic mice [238]. Another technique that uses a shadow mask provided a uniform microneedle fabrication, and it overcame low-throughput-associated issues in the droplet formation. The researchers that used this method evidenced a controlled drug dosage with the optimization of hole width and thickness of the shadow mask [241]. Lin et al. also presented a method for rapidly fabricating a microneedle array mold using UV-cured resin and drawing lithography. They demonstrated the possibility of controlling microneedle height and the aspect ratio by changing the heating time and the volume of resin droplets. In addition, the study proved that the described method shortened the microneedle mold production time by several tens of minutes compared with conventional processes [242].

The electro-drawing method utilizes electrohydrodynamic (EHD) force to draw polymer solution droplets in a non-contact manner [243]. On the other hand, centrifugal drawing uses centrifugal force to deform and elongate materials into a needle-tip shape [244].

In short, all these methods offer the advantage of a low cost and the capability for mass production [165]. Furthermore, these techniques are suitable for producing basic structures such as conical or hollow needles. However, they are limited in their ability to manufacture complex structures because the drawing force during fabrication is typically unidirectional, and incorporating additional materials can be challenging. Table 4 summarizes the benefits and drawbacks of drawing-based methods [165].

**Table 4.** Benefits and drawbacks of drawing-based methods.

| Method | Advantages | Disadvantages |
|---|---|---|
| Mechanical force drawing | Cost effective | Time consuming<br>Low precision<br>Unable to produce complex structures<br>Restricted to thermoplastic materials |
| Contact drawing | Cost effective<br>Rapid | Low precision<br>Unable to produce complex structures<br>Viscosity of basic material requires adjustment |
| Electro-drawing | Cost effective<br>Rapid | Low precision<br>Unable to produce complex structures<br>Conductivity of basic material requires adjustment |
| Centrifugal drawing | Cost effective<br>Rapid | Low precision<br>Unable to produce complex structures |

## 4.6. Atomized Spraying Method

This technique consists of an atomized spray, which can be produced by a nozzle connected to an air source and liquid formulation [168]. For the manufacture of dissolving microneedles, the formulation is filled into PDMS molds and left to dry for 2 h at room temperature. In addition, this method can be used to fabricate laminate-layered and horizontally layered dissolving microneedles [202,204]. This process overcomes the issues linked to the limited capacity for the mass production of dissolving microneedles with the required geometry and physical properties. It also can mitigate issues related to the effects of liquid surface tension and viscosity when filling the microneedle molds [168]. Kim et al. showed that the separate deposition of protein and polymer solutions via the dual-nozzle spray deposition process is capable of manufacturing drug-encapsulated and mechanically stable microneedles [245].

## 4.7. Injection Molding

The standard injection molding process cycle has five phases. In the first phase, a reciprocating screw transports resin pellets from the hopper into the feeding zone of the barrel. In the second phase, which is the end of the plasticizing process, a homogenous melt is available for injection into the cavity. The next phase comprises the injection of the melt into the closed mold, followed by phase four, which is the packing and cooling phase. Packing is essential for compensating the shrinkage of the polymer. Finally, the ejection of the part takes place [246].

Injection molding is another microneedle fabrication method that has the advantage of allowing the mass production of microneedles at a low cost [166]. Furthermore, micro-injection molding offers high repeatability, precise dosing, and elevated injection flow rates by segregating the plasticization and polymer melt injection processes [216]. However, this technique also has limitations, such as difficulty in controlling the small shot size due to the typical size of the screw, which ranges from approximately 15 to 150 mm, as well as the higher initial cost of the equipment [246].

Lhernould et al. developed a hollow polymer microneedle array using poly carbonate material. The fabricated microneedles have been proven to withstand high force and can be used for multiple insertions without blunting the needle [247]. Furthermore, the following has been reported: the manufacture of solid microneedles by the micro-injection molding process and the ability of the needles to deliver hydrophilic high-molecular-weight molecules [248]. Another study described the production of polymeric microneedles by molding plastic material. The fabricated microneedles effectively penetrated a fresh chicken leg and beef liver, extracting approximately 0.04 μL of liquid from these tissues [249].

## 4.8. Micro-Mechanical Machining

This technique involves needle manufacture by using CNC (computer numerical control) milling processes [134]. CNC milling involves the removal of material using a rotating cutter at high speeds. This cutting can be carried out on more than one axis, according to the machine's capacity. The cutting width is defined by machine tools that are separate and reusable accessories of the milling machine [134].

The micro-mechanical machining method can be applied in the preparation of dissolving microneedles through a three-step production process [250]. In the first step, a positive mold is fabricated using a stainless-steel workpiece that is subjected to micromilling. Cutting parameters are acquired using a G-code generated from the CAD drawing. In the second step, PDMS is poured into the fabricated positive mold to be casted as a negative mold. As soon as the PDMS mold is cured, it can be used for the final step of the manufacture of dissolving microneedles. This final stage involves the preparation of a polymer solution, which will be spun cast onto the negative mold to achieve the desired patch of microneedles [250]. This process is advantageous since it comprises mold manufacture from a metal, which has higher structural strength, thus enabling prototyping of high-aspect-ratio needles and varied geometry. On the contrary, this method would be unsustainable in

non-metallic mold materials such as silicon. Moreover, both molds can be used multiple times, providing a large-scale simultaneous fabrication of dissolving microneedles [134].

Malek-Khatabi et al. manufactured master molds using CNC machining for the subsequent production of dissolving microneedles composed of HA and polyvinylpyrrolidone. The researchers concluded that CNC machining enables a fast and cost-effective fabrication of master molds, which facilitates the production of microneedles [251]. Another study reported the fabrication of conical needles by the CNC micromilling process with a base diameter and height of 1 mm by 1 mm [252].

### 4.9. Additive Manufacturing

Lately, additive manufacturing, more commonly known as 3D printing, has rapidly been gaining attention as a means of manufacturing microneedles and molds [166]. In fact, the biomedical device industry has witnessed a swift adoption of 3D printing technologies for tissue engineering implants in recent years [253–258].

All additive manufacturing technologies involve the design of a 3D object with CAD, which is subsequently converted to an STL file to tessellate the 3D shape and slice it into digital layers. The next phase consists of transferring the STL file to the printer via specialized machine software and adjusting the printer settings according to the printing parameters. The model is built by the printer through the fusion or deposition of proper material, such as ceramic, thermoplastic, plastic, liquid, photopolymer, powder, or even living cell material, in layers [259–265].

Additive manufacturing technologies include fused deposition modelling (FDM) [266,267], material jetting (MJ) [268–270], and photopolymerization-based techniques such as stereolithography (SLA) [88,271–276], digital light processing (DLP) [277–280], continuous liquid interface production (CLIP) [281,282], and two-photon polymerization (2PP) [155,283–285]. All these cutting-edge technologies were successfully employed in the manufacture of microneedles, having numerous advantages when comparing with conventional fabrication methods. These advantages comprise a low cost, simplicity, the ability to generate sophisticated geometrical products including alterations to the original designs at any time, and the fabrication of patient-specific devices [168,239,264]. Table 5 summarizes the principal advantages and disadvantages of some additive manufacturing technologies [165].

**Table 5.** Advantages and disadvantages of some additive manufacturing technologies.

| Method | Advantages | Disadvantages |
| --- | --- | --- |
| Fused deposition modelling (FDM) | Cost effective<br>Less time consuming | Low precision<br>Cannot fabricate complex structures<br>Needs post treatment |
| Stereolithography (SLA) | Less time consuming<br>Able to fabricate complex structures | Average precision |
| Two-photon polymerization (2PP) | High precision<br>Easy to fabricate complex structures | Expensive<br>Time consuming<br>Difficult to fabricate objects with large volume |

### 4.9.1. Fused Deposition Modelling (FDM)

The preparation for printing microneedles with typical FDM printers begins with the design of microneedles using CAD software and the optimization of its geometry according to the printer specification [261,265]. Afterwards, the proper thermoplastic material, in filament form, is supplied to the printer through rollers. Here, it is heated to slightly above its softening point (glass transition temperature) by heating elements, rendering it molten. Guided by gears, the molten or softened material is directed toward the printer's head, where it is extruded through a nozzle and deposited layer by layer onto a build plate. This material cools and solidifies in less than a second [168,259–262]. The 3D structures are

created by moving the printer's head in the x- and y-axes, while the platform moves in the z-axis [264].

Typical filaments employed in an FDM printer are acrylonitrile butadiene styrene, poly(lactic acid), poly(vinyl alcohol), high-impact polystyrene, polyethylene terephthalate glycol-modified, and nylon. The filament sizes adopted in the print head available on the market are between 1.75 mm and 2.85–3 mm [261]. Additionally, during an FDM process, it is necessary to optimize the processing parameters such as the nozzle diameter, feed rate, temperature of both the nozzle and the building plate, printing speed, height of the layers, and part-built orientation [262,264].

FDM is a versatile and cost-effective microneedle fabrication method; however, its main issue is low printing resolution [168]. Researchers successfully used FDM to print microneedles that were subsequently coated [266]. Luzuriaga et al. described the development of ideally sized and shaped needles through a combination of FDM with a post-fabrication etching step [267]. Wu et al. optimized a methodology for the fabrication of poly(lactic acid) microneedles with tailored structures, involving the FDM process [286]. The study demonstrated that the increase in the thermal parameters during the FDM process can improve the interfacial bonding strength and decrease the void density of the poly(lactic acid) layers, within the temperature range that the FDM printer and poly(lactic acid) filament can withstand. In addition, the detachment of the poly(lactic acid) needles and collapse of the substrates during etching can be efficiently prevented by the optimized poly(lactic acid) needle array [286]. Researchers developed a novel, simple, fast, and reliable method for microneedle mold manufacture by employing 3D FDM printing technology [287]. They evidenced the great advantages of this technology that allows a faster production, requires less ingredients, introduces the use of poly(lactic acid) as a GRAS material for the fabrication of molds, and does not require the production of master templates. The study also revealed the possibility of applying this method in the fabrication of polymeric microneedles of various geometries for enhancing transdermal delivery of galantamine and probably other APIs [287].

### 4.9.2. Material Jetting (MJ)

MJ is a material deposition method that adopts an identical printing process as FDM, in which the prototype is manufactured in a layer-by-layer manner [288]. Unlike FDM, MJ relies on thermal or piezoelectric print heads to deposit liquid building material drop by drop at high speed [264]. The primary ink used for MJ is UV curable ink, which necessitates brief exposure to UV light for curing before the next layer can be deposited. This cycle repeats until the entire model is constructed [288].

Compared to other 3D printing techniques, MJ has a lower resolution, which is why it is predominantly favored for coating the surface of microneedles with drugs, rather than the direct manufacture of microneedles. The dispenser in such printers is often driven by piezoelectricity. Here, voltage pulses interact with a piezoelectric material, generating an electric field that prompts the nozzle to release minute droplets in the picoliter range, typically between 1 and 70 pL [268]. In this way, it is possible to control in a uniform and reproducible way the dosage of drugs coated onto microneedles. It has been reported by identical studies that 300 pL of insulin coating formulations was uniformly coated onto SLA-printed microneedles using MJ printing without any wastage [88,273]. Uddin et al. also used MJ printing to coat metal microneedles with an anticancer drug formulation [289]. Another research team incorporated MJ printing into the production of drug-loaded microneedles, employing piezoelectric dispensing to precisely dispense a controlled volume of a drug formulation directly into PDMS molds [268].

MJ and FDM have an advantage in common that is the ability to print with varied materials simultaneously due to the availability of numerous print heads, increasing the versatility of the printed microneedles [288]. A study described the manufacture of hollow microneedles with a support material by an MJ 3D printer to obtain the high resolution of the microneedles [269]. Derakhshandeh et al. evidenced the capability to fabricate

support structures using sacrificial materials, which can be dissolved in chemicals such as sodium hydroxide for removal. This method offers greater flexibility in printing small, intricate structures where conventional breakaway support removal is not feasible. This is particularly useful when the tiny support structures are needed to bolster the complex structures of individual microneedles or when the support structures are embedded within the microneedle structure itself. Consequently, it becomes feasible to print cavities in the microneedles with diameters ranging from 200 to 500 μm, as the printing process can be executed with support material [269,288]. Barnun et al. also created microneedles with cavities using the support material, which was removed from the cavities and then replaced by model drug-containing hydrogels through pipetting with a special attachment [270].

### 4.9.3. Stereolithography (SLA)

SLA stands as the prevailing technology for microneedle printing, offering exceptional resolution and accuracy alongside a smooth surface finish [168]. This process essentially involves the photopolymerization of liquid resin containing photo-active monomers under UV light. Microneedles are created through the solidification of successive layers of resin, facilitated by high-energy light such as a UV laser beam directed by scanner mirrors [261]. A microneedle pattern is generated by a laser beam on the surface of a resin that causes the resin to have definite depth. Finally, microneedles are washed in an alcohol bath to remove unpolymerized resin residues and then cured in the UV chamber [88,273]. SLA achieves high-quality parts with a fine resolution (typically around 10 μm), but it is a relatively slow and expensive process. Additionally, the range of available printing materials is limited by the lack of biocompatibility [290].

This technology has been used in the fabrication of microneedles, including solid microneedles [276], hollow microneedles [271], and molds [274]. Different studies have documented the utilization of SLA technology in producing arrays of microneedles. These microneedles were manufactured using a Class 1 biocompatible resin known for its outstanding mechanical strength. Subsequently, the microneedles were coated with insulin–sugar films [88,273]. Yadav et al. printed hollow microneedles using SLA technology, achieving objects with high resolution and high fidelity, as confirmed by optical and electron microscopy image evaluations. Furthermore, the researchers demonstrated that the developed microneedles were mechanically robust and suitable for penetration through porcine skin tissue, thus depositing a rifampicin solution efficiently into the skin tissue [291]. Choo et al. revealed that high-resolution and high-dimensional microneedles were fabricated by adjusting the printing angle of an SLA-type 3D printer. They realized that when the printing angle was set to 60° for the x- and y-axes, the single stacking layer area, including the microneedle tip, was the largest, and the microneedle with the sharpest tip was printed [292]. Another study reported the fabrication of a microneedle platform using an SLA 3D printer, varying the 3D printing angle and aspect ratio. The investigators concluded that the optimal printing angle was 30°, resulting in needle tip and base diameters of ≈50 and ≈330 μm and heights of ≈550/850/1180 μm [293]. Yang et al. developed 3D-printed morphology-customized microneedles with excellent transdermal drug delivery efficiency [294]. They demonstrated the success of the SLA technique in designing and manufacturing sophisticated morphology-customized microneedles. Additionally, the employed technology guaranteed a suitable mechanical strength of the microneedles including the penetration force and fracture force. In turn, the results of drug loading capacity and drug release profiles evidenced that transdermal microneedles could be well programmed with sophisticated morphologies and predesigned surface areas to achieve both sufficient drug loading capacity and desired drug release profiles [294]. Turner et al. developed a transdermal drug delivery microneedle platform that exhibits successful skin penetration, provides an effective controlled drug release, and is manufactured by a quick, low-cost, flexible SLA 3D printing micromolding process [295]. In fact, they fabricated 3D-printed microneedle templates, which were optimized and used in a micromolding process to form negative PDMS molds, which subsequently were used in the manufac-

ture of hydrogel-forming microneedles. This study also evidenced a comparison between the developed microneedles and commercially available microneedle molds, which were produced by laser-etch molding, in terms of porcine skin penetration performance. In this way, a comparable performance was demonstrated between the two with a difference of a 9% penetration rate in microneedle penetration at the minimum penetrative force required [295].

4.9.4. Digital Light Processing (DLP)

DLP also relies on photopolymerization but operates by polymerizing photosensitive polymers through light projections. Compared to SLA, DLP is faster, employing a high-definition projector that illuminates the entire cross-section of the object at once, in the form of volumetric pixels [259].

DLP can be employed in the manufacture of microneedles. Indeed, the following has been reported: the application of DLP in printing solid microneedle array structures with several geometries out of an acrylate-based polymer for wound healing applications [277]. Another study demonstrated the successful manufacture of microneedle molds for nanoparticle delivery using a desktop DLP 3D printer [279]. Lu et al. used a microstereolithographic (DLP) apparatus to manufacture drug-loaded microneedle arrays for the transdermal delivery of a chemotherapeutic drug [278]. Yao et al. developed hydrogel microneedles using a high-precision digital light processing 3D printing system. The researchers evidenced the benefits of using the described method, such as the fact that it is low-cost and fast, providing good mechanical performance, drug injection, and drug detection ability of microneedles [296]. Mathew et al. employed the DLP method in the fabrication of hollow microneedles using commercial UV curable resin. They successfully developed hollow microneedles with good mechanical strength and resistance to compression [297]. The following has also been reported: the manufacture of silk fibroin microneedles by DLP 3D printing of a silk fibroin solution with riboflavin as an enzymatic photoinitiator. In the study, oblique and sharp microneedles were achieved using an anti-aliasing strategy and shrinkage of the hydrogel in a dehydration process. Furthermore, the developed microneedles were strong and showed no severe damage to the structure upon the application of $\approx 300$ mN of compressive stress [298]. Sachan et al. successfully fabricated solid microneedle arrays by DLP-based 3D printing of polytetrafluoroethylene. The developed microneedles showed their ability to penetrate discarded human skin [299]. Wu et al. also used DLP 3D printing technology to simply fabricate sharp microneedles (tip radius < 6 μm) [300]. Monou et al. manufactured hollow microneedle devices using DLP printing technology. Through imaging studies, the researchers demonstrated the excellent printability of the material and confirmed the high fidelity of the printed objects compared to their corresponding CAD models [301]. Another study used DLS technology to develop gelatin methacryloyl microneedles containing amoxicillin. A SEM analysis uncovered microneedles with sharp tips, meeting the desired dimensions and displaying consistent morphology. Mechanical testing demonstrated no discontinuity or breakage even at a displacement of 300 μm. Additionally, the developed microneedles demonstrated a rapid release of amoxicillin within the first 6 h of incubation [302].

4.9.5. Continuous Liquid Interface Production (CLIP)

Like DLP, CLIP utilizes UV light projection for printing. However, the key distinction lies in the continuous printing process of CLIP, as opposed to the stepwise layer-by-layer approach of DLP. This enables CLIP to achieve printing speeds approximately 100 times faster than DLP [303]. A permeable window at the bottom of the resin tank allows oxygen, which hinders photopolymerization, to continuously permeate through. This process creates a "dead zone". Given this "dead zone", the printing process becomes continuous because the printed structure remains unattached to the resin tray, eliminating the need for delamination from the tray. Furthermore, the prototypes manufactured from CLIP do not have the stair-stepping effect seen in DLP because of the continuous printing process [288].

As a result of the advantage of being a continuous printing process, CLIP is a favorable choice in printing complex structures compared to SLA or DLP technologies [288]. Rajesh et al. demonstrated this fact by employing high-resolution CLIP to print sophisticated microneedles with a novel design. These dimensions were challenging to replicate via material deposition, and the properties were difficult to achieve with SLA and DLP due to the delamination process. This research team manufactured square pyramidal microneedles with lattice structures and showed their ability to trap liquid for drug delivery [304]. Johnson et al. used CLIP to rapidly prototype sharp microneedles with tunable geometries. The square pyramidal CLIP microneedles effectively pierced murine skin ex vivo and released the fluorescent drug surrogate rhodamine [281]. Caudill et al. designed and 3D printed faceted polymeric microneedles by CLIP technology for vaccine formulation and transdermal delivery. Their model vaccine exhibited efficient ID delivery of vaccine components as well as the induction of potent and balanced humoral and cellular immunity [282].

4.9.6. Two-Photon Polymerization (2PP)

2PP is an economical fabrication process that builds 3D structures layer by layer from solid, liquid, or powder precursors, at the microscale and nanoscale [168]. The polymerization into microneedle structure occurs through the focus of a femtosecond or picosecond laser into a liquid resin droplet [209,259]. This method involves the temporal and spatial overlapping of photons to induce photopolymerization [283]. The benefits of the 2PP technique include its high degree of flexibility, scalable resolution, improved control over geometry, and ability to be executed in conventional facilities [209,259].

A study reported the use of 2PP in the manufacture of microneedle Ormocer$^{®}$ (organically modified ceramic) materials [305]. A group of researchers also used 2PP to produce hollow microneedles combined with internal laser-generated microchannels [284]. Aksit et al. employed 2PP in the printing of ultra-sharp polymer microneedles [285]. Another research group described an approach to produce high-quality microneedle master templates by 2PP [155]. Gittard et al. proposed the production of microneedles using 2PP, allowing for a broad spectrum of geometries including in-plane, out-of-plane, rocket-shaped, and mosquito-fascicle-shaped microneedles [283]. Rad et al. fabricated ultra-sharp microneedles with microfluidic channels using 2PP, which enables flexible designs with resolution down to 100 nm. In fact, the investigators employed 2PP in the manufacture of master molds from which elastomeric negative molds have been used in a rapid micro-molding technique to make batches of ultra-sharp microneedles [306]. Pillai et al. reported the development of microneedle master templates using the 2PP method. They described a one-step process for fabricating high-quality, reusable, and long-lasting microneedle templates that allows an easy replication of negative PDMS molds [307]. Fakeih et al. created three microneedle designs with a constant pore size and controlled pore locations using 2PP [308]. He et al. also used 2PP to print structures with sub-100 nm resolution [309].

## 5. Microneedle System Applications

The use of microneedles has been expanded to numerous fields, such as drug and vaccine delivery, therapy, cosmetics, diagnoses, cancer research, tissue engineering, wound healing, and sample extraction. Table 6 describes examples of the main applications of microneedles.

**Table 6.** Usage of microneedle systems.

| Microneedle System | Active Ingredient/Sampling | Application | Reference |
| --- | --- | --- | --- |
| Polymeric microneedles | Ovalbumin and CpG | Vaccine delivery | [285] |
| Hollow microneedles | Insulin | Vaccine delivery | [310] |
| Dissolving microneedle patches | Heat-inactivated bacteria | Vaccine delivery | [311] |
| Solid pyramidal microneedle | Stabilized HIV envelope trimer immunogen and adjuvant | Vaccine delivery | [312] |
| Microneedle patches | Acetyl-hexapeptide-3 | Wrinkle | [280] |
| Stainless solid microneedles | 5-Fluorouracil | Keloids | [313] |
| Poly(ionic liquid)-based microneedle patches | Salicylic acid | Acne | [314] |
| Dissolvable hyaluronic acid microneedles | Shikonin | Hypertrophic scars | [315] |
| Methacrylate gelatin/polyethylene glycol diacrylate double-network hydrogel microneedle patch | Betamethasone | Hypertrophic scars | [316] |
| Dissolving microneedle array | MiRNA-modified functional exosomes | Hypertrophic scars | [317] |
| Dissolving gelatin and starch microneedle patches | Losartan | Hypertrophic scars | [318] |
| Dissolving microneedle | Triamcinolone acetonide | Psoriasis | [50] |
| Dissolving microneedle patches | Tetramethylpyrazine | Rheumatoid arthritis | [319] |
| Hydrogen peroxide-responsive microneedle | Integrin $\alpha_v\beta_6$-blocking antibody | Pulmonary fibrosis | [320] |
| Dissolvable microneedles | Dexamethasone | Atopic dermatitis | [321] |
| Natural antimicrobial material microneedles | Peony leaf extract | Chronic wounds | [322] |
| Hyaluronic acid microneedle | Recombinant humanized collagen type III and naproxen loaded poly(lactic-co-glycolic acid) nanoparticle | Chronic wounds | [323] |
| Zwitterionic microneedle dressings | Zinc oxide nanoparticles and asiaticoside | Chronic wounds | [324] |
| Encoded structural color microneedle patches | Photonic crystals | Wound biomarker detection | [325] |
| Microneedle patches | Interstitial fluid | Sampling of interstitial fluid | [326] |
| Microfluidic-based wearable plasmonic microneedle sensor | Interstitial fluid | Uric acid monitoring | [327] |
| Polymeric-microneedle-coupled electrochemical sensor array | Interstitial fluid | Diagnosis of chronic kidney disease | [328] |
| Ion-conductive porous microneedle-based glucose sensing device combined with reverse ion electroosmosis | Interstitial fluid | Glucose determination (management of chronic diseases) | [329] |
| Gelatin methacrylate–acrylic acid microneedle patch | Interstitial fluid | Breast cancer screening | [330] |
| Hydrogel microneedles | Interstitial fluid | Colorectal cancer diagnosis | [331] |
| AdminPen™ hollow microneedle array | Hypericin lipid nanocapsules | Non-melanoma skin cancer | [332] |
| Dissolvable microneedle patch | Resveratrol nanocrystals and fluorouracil@hydroxypropyl-beta-cyclodextrin | Cutaneous melanoma | [333] |
| Hydrothermally responsive multi-round acturable microneedle | Docetaxel | Subcutaneous tumors | [334] |

Delivering drugs through the stratum corneum is a minimally invasive approach made possible by microneedle devices. These devices are used not only for administering vaccines [285,310–312] but also for treating various conditions like psoriasis [50] and rheumatoid arthritis [319], as outlined in Table 6. Microneedle-based drug delivery has also gained attention in cancer research, with melanoma—one of the most common types of skin cancer—being a key focus area. These systems offer a promising way to deliver anticancer agents effectively for melanoma treatment [333].

In addition, microneedles are changing the landscape of medical diagnostics and therapy monitoring. Traditional methods for assessing biomarkers in the body are often painful and require specialized equipment. Microneedle technology, however, provides a simpler and less intrusive alternative. The collection of interstitial fluid through microneedles is both cost-effective and quicker compared to other techniques. This innovation enhances biosensing capabilities by enabling efficient transdermal sampling, offering a versatile method to detect a range of analytes in interstitial fluid, which aids in disease diagnoses [326–331].

Microneedles are also proving to be effective in cosmetic applications, helping to treat skin lesions [313,315–318], acne vulgaris [314], and wrinkles [280]. Their minimally invasive nature and ability to promote transdermal absorption make them an attractive option for various medical and cosmetic applications.

## 6. Conclusions

The urgent need for a new and versatile technology that crosses the boundaries between invasive and non-invasive treatments has led to the emergence of microneedle systems, whose efficiency as a biomedical device has attracted enormous attention from the industry and academic research communities.

Over the past few years, there has been significant progress in the field of microneedles. This is not only in terms of microneedle compositions and morphologies, but also in the wide range of applications, including drug delivery, vaccinees, patients' fluid collection (point-of-care diagnostics), and biosignal acquisition, among others.

Microneedles as innovative devices offer several advantages, such as effectiveness, portability, and precision. It is noteworthy that the material selection, microneedle design, and manufacturing process are key elements for the device success in any application.

The present review provides a comprehensive guide for the design of a successful microneedle system, as it presents and discusses all the parameters that need to be met to achieve the goal, an efficient medical device. It is necessary to clearly identify the need or application and design the system taking into consideration needles' length, diameter, ratios, and materials, as well as the method of preparation. All the described parameters must be carefully designed.

The versatility of microneedle systems provided by their different structures, designs, and preparation methods allows them to be applied in a wide range of fields successfully.

**Conflicts of Interest:** Authors Nelson Oliveira and Sónia Ferreira were employed by the company BestHealth4U Lda. The remaining authors declare that the research was conducted in the absence of any commercial or financial relationships that could be construed as a potential conflict of interest.

## References

1. Chuong, C.M.; Nickoloff, B.J.; Elias, P.M.; Goldsmith, L.A.; Macher, E.; Maderson, P.A.; Sundberg, J.P.; Tagami, H.; Plonka, P.M.; Thestrup-Pedersen, K.; et al. What is the "true" function of skin? *Exp. Dermatol.* **2002**, *11*, 159–160. [CrossRef]
2. Chien, Y.W.; Liu, J.-C. Transdermal Drug Delivery Systems. *J. Biomater. Appl.* **1986**, *1*, 183–206. [CrossRef]
3. Wong, W.F.; Ang, K.P.; Sethi, G.; Looi, C.Y. Recent Advancement of Medical Patch for Transdermal Drug Delivery. *Medicina* **2023**, *59*, 778. [CrossRef]
4. Lasagna, L.; Greenblatt, D.J. More Than Skin Deep: Transdermal Drug-Delivery Systems. *N. Engl. J. Med.* **1986**, *314*, 1638–1639. [CrossRef]
5. Zhou, Q.; Li, H.; Liao, Z.; Gao, B.; He, B. Bridging the Gap between Invasive and Noninvasive Medical Care: Emerging Microneedle Approaches. *Anal. Chem.* **2023**, *95*, 515–534. [CrossRef]
6. Waghule, T.; Singhvi, G.; Dubey, S.K.; Pandey, M.M.; Gupta, G.; Singh, M.; Dua, K. Microneedles: A smart approach and increasing potential for transdermal drug delivery system. *Biomed. Pharmacother.* **2019**, *109*, 1249–1258. [CrossRef]
7. Pettis, R.J.; Harvey, A.J.; Ham, A.S.; Buckheit, R.W.; Singla, S.K.; Sachdeva, V.; Shin, C.I.; Jeong, S.D.; Rejinold, N.S.; Kim, Y.-C.; et al. Microneedle delivery: Clinical studies and emerging medical applications. *Ther. Deliv.* **2012**, *3*, 357–371. [CrossRef]
8. Al-Japairai, K.A.S.; Mahmood, S.; Almurisi, S.H.; Venugopal, J.R.; Hilles, A.R.; Azmana, M.; Raman, S. Current trends in polymer microneedle for transdermal drug delivery. *Int. J. Pharm.* **2020**, *587*, 119673. [CrossRef]
9. Yan, G.; Warner, K.S.; Zhang, J.; Sharma, S.; Gale, B.K. Evaluation needle length and density of microneedle arrays in the pretreatment of skin for transdermal drug delivery. *Int. J. Pharm.* **2010**, *391*, 7–12. [CrossRef] [PubMed]
10. Xu, J.; Xu, D.; Xuan, X.; He, H. Advances of Microneedles in Biomedical Applications. *Molecules* **2021**, *26*, 5912. [CrossRef] [PubMed]
11. Sachan, A.; Sachan, R.J.; Lu, J.; Sun, H.; Jin, Y.J.; Erdmann, D.; Zhang, J.Y.; Narayan, R.J. Injection molding for manufacturing of solid poly(l-lactide-co-glycolide) microneedles. *MRS Adv.* **2021**, *6*, 61–65. [CrossRef]
12. Jin, X.; Zhu, D.D.; Chen, B.Z.; Ashfaq, M.; Guo, X.D. Insulin delivery systems combined with microneedle technology. *Adv. Drug Deliv. Rev.* **2018**, *127*, 119–137. [CrossRef] [PubMed]
13. Luo, X.; Yu, Q.; Liu, Y.; Gai, W.; Ye, L.; Yang, L.; Cui, Y. Closed-Loop Diabetes Minipatch Based on a Biosensor and an Electroosmotic Pump on Hollow Biodegradable Microneedles. *ACS Sens.* **2022**, *7*, 1347–1360. [CrossRef] [PubMed]
14. Han, D.; Morde, R.S.; Mariani, S.; La Mattina, A.A.; Vignali, E.; Yang, C.; Barillaro, G.; Lee, H. 4D Printing of a Bioinspired Microneedle Array with Backward-Facing Barbs for Enhanced Tissue Adhesion. *Adv. Funct. Mater.* **2020**, *30*, 1909197. [CrossRef]
15. Kim, Y.-C.; Park, J.-H.; Prausnitz, M.R. Microneedles for drug and vaccine delivery. *Adv. Drug Deliv. Rev.* **2012**, *64*, 1547–1568. [CrossRef] [PubMed]
16. Lee, G.; Ma, Y.; Lee, Y.-H.; Jung, H. Clinical Evaluation of a Low-pain Long Microneedle for Subcutaneous Insulin Injection. *BioChip J.* **2018**, *12*, 309–316. [CrossRef]
17. Zhang, R.; Miao, Q.; Deng, D.; Wu, J.; Miao, Y.; Li, Y. Research progress of advanced microneedle drug delivery system and its application in biomedicine. *Colloids Surf. B Biointerfaces* **2023**, *226*, 113302. [CrossRef]
18. Parhi, R. Recent advances in 3D printed microneedles and their skin delivery application in the treatment of various diseases. *J. Drug Deliv. Sci. Technol.* **2023**, *84*, 104395. [CrossRef]
19. Yang, G.; Chen, Q.; Wen, D.; Chen, Z.; Wang, J.; Chen, G.; Wang, Z.; Zhang, X.; Zhang, Y.; Hu, Q.; et al. A Therapeutic Microneedle Patch Made from Hair-Derived Keratin for Promoting Hair Regrowth. *ACS Nano* **2019**, *13*, 4354–4360. [CrossRef] [PubMed]
20. Barnum, L.; Samandari, M.; Schmidt, T.A.; Tamayol, A. Microneedle arrays for the treatment of chronic wounds. *Expert Opin. Drug Deliv.* **2020**, *17*, 1767–1780. [CrossRef]
21. Than, A.; Liu, C.; Chang, H.; Duong, P.K.; Cheung, C.M.G.; Xu, C.; Wang, X.; Chen, P. Self-implantable double-layered micro-drug-reservoirs for efficient and controlled ocular drug delivery. *Nat. Commun.* **2018**, *9*, 4433. [CrossRef] [PubMed]
22. Ju, E.; Peng, M.; Xu, Y.; Wang, Y.; Zhou, F.; Wang, H.; Li, M.; Zheng, Y.; Tao, Y. Nanozyme-integrated microneedle patch for enhanced therapy of cutaneous squamous cell carcinoma by breaking the gap between $H_2O_2$ self-supplying chemodynamic therapy and photothermal therapy. *J. Mater. Chem. B* **2023**, *11*, 6595–6602. [CrossRef] [PubMed]
23. Shukla, S.; Mamale, K.B.; Arya, R.K.; Kaundal, R.K.; Shukla, R. Therapeutic potential of microneedles based delivery systems for the management of atopic dermatitis. *J. Drug Deliv. Sci. Technol.* **2023**, *84*, 104493. [CrossRef]
24. Cheng, X.; Hu, S.; Cheng, K. Microneedle Patch Delivery of PROTACs for Anti-Cancer Therapy. *ACS Nano* **2023**, *17*, 11855–11868. [CrossRef] [PubMed]
25. Li, W.; Chen, J.Y.; Terry, R.N.; Tang, J.; Romanyuk, A.; Schwendeman, S.P.; Prausnitz, M.R. Core-shell microneedle patch for six-month controlled-release contraceptive delivery. *J. Control. Release* **2022**, *347*, 489–499. [CrossRef] [PubMed]
26. Kim, Y.; Park, I.H.; Shin, J.; Choi, J.; Jeon, C.; Jeon, S.; Shin, J.; Jung, H. Sublingual Dissolving Microneedle (SLDMN)-based Vaccine for Inducing Mucosal Immunity Against SARS-CoV-2. *Adv. Healthc. Mater.* **2023**, *12*, 2300889. [CrossRef] [PubMed]
27. Wang, L.; Yang, L.; Zhang, F.; Liu, X.; Xie, Q.; Liu, Q.; Yuan, L.; Zhao, T.; Xie, S.; Xu, Q.; et al. A microneedle-based delivery system for broad-protection seasonal influenza A DNA nanovaccines. *Cell Rep. Phys. Sci.* **2023**, *4*, 101430. [CrossRef]

28. Friedel, M.; Werbovetz, B.; Drexelius, A.; Watkins, Z.; Bali, A.; Plaxco, K.W.; Heikenfeld, J. Continuous molecular monitoring of human dermal interstitial fluid with microneedle-enabled electrochemical aptamer sensors. *Lab Chip* **2023**, *23*, 3289–3299. [CrossRef] [PubMed]

29. Chen, J.; Cai, X.; Zhang, W.; Zhu, D.; Ruan, Z.; Jin, N. Fabrication of Antibacterial Sponge Microneedles for Sampling Skin Interstitial Fluid. *Pharmaceutics* **2023**, *15*, 1730. [CrossRef]

30. Alimardani, V.; Abolmaali, S.S.; Yousefi, G.; Rahiminezhad, Z.; Abedi, M.; Tamaddon, A.; Ahadian, S. Microneedle Arrays Combined with Nanomedicine Approaches for Transdermal Delivery of Therapeutics. *J. Clin. Med.* **2021**, *10*, 181. [CrossRef]

31. Li, Q.Y.; Zhang, J.N.; Chen, B.Z.; Wang, Q.L.; Guo, X.D. A solid polymer microneedle patch pretreatment enhances the permeation of drug molecules into the skin. *RSC Adv.* **2017**, *7*, 15408–15415. [CrossRef]

32. de Groot, A.M.; Platteel, A.C.M.; Kuijt, N.; van Kooten, P.J.S.; Vos, P.J.; Sijts, A.J.A.M.; van der Maaden, K. Nanoporous Microneedle Arrays Effectively Induce Antibody Responses against Diphtheria and Tetanus Toxoid. *Front. Immunol.* **2017**, *8*, 1789. [CrossRef] [PubMed]

33. Kim, J.K.; Roh, M.R.; Park, G.; Kim, Y.J.; Jeon, I.K.; Chang, S.E. Fractionated microneedle radiofrequency for the treatment of periorbital wrinkles. *J. Dermatol.* **2013**, *40*, 172–176. [CrossRef] [PubMed]

34. Abiandu, I.; Ita, K. Transdermal delivery of potassium chloride with solid microneedles. *J. Drug Deliv. Sci. Technol.* **2019**, *53*, 101216. [CrossRef]

35. Bollella, P.; Sharma, S.; Cass, A.E.G.; Antiochia, R. Minimally-invasive Microneedle-based Biosensor Array for Simultaneous Lactate and Glucose Monitoring in Artificial Interstitial Fluid. *Electroanalysis* **2019**, *31*, 374–382. [CrossRef]

36. Senel, M.; Dervisevic, M.; Voelcker, N.H. Gold microneedles fabricated by casting of gold ink used for urea sensing. *Mater. Lett.* **2019**, *243*, 50–53. [CrossRef]

37. Bhadale, R.S.; Londhe, V.Y. Solid microneedle assisted transepidermal delivery of iloperidone loaded film: Characterization and Skin deposition studies. *J. Drug Deliv. Sci. Technol.* **2023**, *79*, 104028. [CrossRef]

38. van der Maaden, K.; Yu, H.; Sliedregt, K.; Zwier, R.; Leboux, R.; Oguri, M.; Kros, A.; Jiskoot, W.; Bouwstra, J.A. Nanolayered chemical modification of silicon surfaces with ionizable surface groups for pH-triggered protein adsorption and release: Application to microneedles. *J. Mater. Chem. B* **2013**, *1*, 4466–4477. [CrossRef] [PubMed]

39. Meyer, B.K.; Kendall, M.A.; Williams, D.M.; Bett, A.J.; Dubey, S.; Gentzel, R.C.; Casimiro, D.; Forster, A.; Corbett, H.; Crichton, M.; et al. Immune response and reactogenicity of an unadjuvanted intradermally delivered human papillomavirus vaccine using a first generation Nanopatch™ in rhesus macaques: An exploratory, pre-clinical feasibility assessment. *Vaccine X* **2019**, *2*, 100030. [CrossRef]

40. Daddona, P.E.; Matriano, J.A.; Mandema, J.; Maa, Y.-F. Parathyroid Hormone (1-34)-Coated Microneedle Patch System: Clinical Pharmacokinetics and Pharmacodynamics for Treatment of Osteoporosis. *Pharm. Res.* **2010**, *28*, 159–165. [CrossRef]

41. Ross, S.; Scoutaris, N.; Lamprou, D.; Mallinson, D.; Douroumis, D. Inkjet printing of insulin microneedles for transdermal delivery. *Drug Deliv. Transl. Res.* **2015**, *5*, 451–461. [CrossRef] [PubMed]

42. Cormier, M.; Johnson, B.; Ameri, M.; Nyam, K.; Libiran, L.; Zhang, D.D.; Daddona, P. Transdermal delivery of desmopressin using a coated microneedle array patch system. *J. Control. Release* **2004**, *97*, 503–511. [CrossRef] [PubMed]

43. Al Sulaiman, D.; Chang, J.Y.H.; Bennett, N.R.; Topouzi, H.; Higgins, C.A.; Irvine, D.J.; Ladame, S. Hydrogel-Coated Microneedle Arrays for Minimally Invasive Sampling and Sensing of Specific Circulating Nucleic Acids from Skin Interstitial Fluid. *ACS Nano* **2019**, *13*, 9620–9628. [CrossRef] [PubMed]

44. Matadh, A.V.; Jakka, D.; Pragathi, S.; Poornima, K.; Shivakumar, H.; Murthy, R.N.; Rangappa, S.; Shivanna, M.; Murthy, S.N. Polymer coated polymeric microneedles for intravitreal delivery of dexamethasone. *Exp. Eye Res.* **2023**, *231*, 109467. [CrossRef] [PubMed]

45. Han, J.H.; Kim, C.R.; Min, C.H.; Kim, M.J.; Kim, S.-N.; Ji, H.B.; Bin Yoon, S.; Lee, C.; Bin Choy, Y. Microneedles coated with composites of phenylboronic acid-containing polymer and carbon nanotubes for glucose measurements in interstitial fluids. *Biosens. Bioelectron.* **2023**, *238*, 115571. [CrossRef] [PubMed]

46. Ramöller, I.K.; Tekko, I.A.; McCarthy, H.O.; Donnelly, R.F. Rapidly dissolving bilayer microneedle arrays—A minimally invasive transdermal drug delivery system for vitamin B12. *Int. J. Pharm.* **2019**, *566*, 299–306. [CrossRef] [PubMed]

47. Chen, Y.-H.; Lai, K.-Y.; Chiu, Y.-H.; Wu, Y.-W.; Shiau, A.-L.; Chen, M.-C. Implantable microneedles with an immune-boosting function for effective intradermal influenza vaccination. *Acta Biomater.* **2019**, *97*, 230–238. [CrossRef]

48. Dillon, C.; Hughes, H.; O'Reilly, N.J.; Allender, C.J.; Barrow, D.A.; McLoughlin, P. Dissolving microneedle based transdermal delivery of therapeutic peptide analogues. *Int. J. Pharm.* **2019**, *565*, 9–19. [CrossRef]

49. Disphanurat, W.; Sivapornpan, N.; Srisantithum, B.; Leelawattanachai, J. Efficacy of a triamcinolone acetonide-loaded dissolving microneedle patch for the treatment of hypertrophic scars and keloids: A randomized, double-blinded, placebo-controlled split-scar study. *Arch. Dermatol. Res.* **2023**, *315*, 989–997. [CrossRef]

50. Wang, H.; Fu, Y.; Liu, P.; Qu, F.; Du, S.; Li, Y.; Du, H.; Zhang, L.; Tao, J.; Zhu, J. Supramolecular Dissolving Microneedle Patch Loading Hydrophobic Glucocorticoid for Effective Psoriasis Treatment. *ACS Appl. Mater. Interfaces* **2023**, *15*, 15162–15171. [CrossRef]

51. Lin, S.; Quan, G.; Hou, A.; Yang, P.; Peng, T.; Gu, Y.; Qin, W.; Liu, R.; Ma, X.; Pan, X.; et al. Strategy for hypertrophic scar therapy: Improved delivery of triamcinolone acetonide using mechanically robust tip-concentrated dissolving microneedle array. *J. Control. Release* **2019**, *306*, 69–82. [CrossRef] [PubMed]

52. Yang, H.; Kim, S.; Jang, M.; Kim, H.; Lee, S.; Kim, Y.; Eom, Y.A.; Kang, G.; Chiang, L.; Baek, J.H.; et al. Two-phase delivery using a horse oil and adenosine-loaded dissolving microneedle patch for skin barrier restoration, moisturization, and wrinkle improvement. *J. Cosmet. Dermatol.* **2019**, *18*, 936–943. [CrossRef] [PubMed]

53. Nguyen, H.X.; Bozorg, B.D.; Kim, Y.; Wieber, A.; Birk, G.; Lubda, D.; Banga, A.K. Poly (vinyl alcohol) microneedles: Fabrication, characterization, and application for transdermal drug delivery of doxorubicin. *Eur. J. Pharm. Biopharm.* **2018**, *129*, 88–103. [CrossRef] [PubMed]

54. Dong, L.; Li, Y.; Li, Z.; Xu, N.; Liu, P.; Du, H.; Zhang, Y.; Huang, Y.; Zhu, J.; Ren, G.; et al. Au Nanocage-Strengthened Dissolving Microneedles for Chemo-Photothermal Combined Therapy of Superficial Skin Tumors. *ACS Appl. Mater. Interfaces* **2018**, *10*, 9247–9256. [CrossRef] [PubMed]

55. Huh, I.; Kim, S.; Yang, H.; Jang, M.; Kang, G.; Jung, H. Effects of two droplet-based dissolving microneedle manufacturing methods on the activity of encapsulated epidermal growth factor and ascorbic acid. *Eur. J. Pharm. Sci.* **2018**, *114*, 285–292. [CrossRef]

56. Hamdan, I.M.; Tekko, I.A.; Matchett, K.B.; Arnaut, L.G.; Silva, C.S.; McCarthy, H.O.; Donnelly, R.F. Intradermal Delivery of a Near-Infrared Photosensitizer Using Dissolving Microneedle Arrays. *J. Pharm. Sci.* **2018**, *107*, 2439–2450. [CrossRef] [PubMed]

57. Li, Y.; Liu, F.; Su, C.; Yu, B.; Liu, D.; Chen, H.-J.; Lin, D.-A.; Yang, C.; Zhou, L.; Wu, Q.; et al. Biodegradable Therapeutic Microneedle Patch for Rapid Antihypertensive Treatment. *ACS Appl. Mater. Interfaces* **2019**, *11*, 30575–30584. [CrossRef] [PubMed]

58. Choi, H.; Hong, J.; Seo, Y.; Joo, S.; Lim, H.; Lahiji, S.F.; Kim, Y. Self-Assembled Oligopeptoplex-Loaded Dissolving Microneedles for Adipocyte-Targeted Anti-Obesity Gene Therapy. *Adv. Mater.* **2024**, *36*, 2309920. [CrossRef]

59. Wan, W.; Li, Y.; Wang, J.; Jin, Z.; Xin, W.; Kang, L.; Wang, J.; Li, X.; Cao, Y.; Yang, H.; et al. PLGA Nanoparticle-Based Dissolving Microneedle Vaccine of *Clostridium perfringens ε* Toxin. *Toxins* **2023**, *15*, 461. [CrossRef]

60. Jiang, X.; Chen, P.; Niu, W.; Fang, R.; Chen, H.; An, Y.; Wang, W.; Jiang, C.; Ye, J. Preparation and evaluation of dissolving tofacitinib microneedles for effective management of rheumatoid arthritis. *Eur. J. Pharm. Sci.* **2023**, *188*, 106518. [CrossRef]

61. Xie, J.; Zhu, X.; Wang, M.; Liu, C.; Ling, G.; Zhang, P. Dissolving microneedle-mediated transdermal delivery of flurbiprofen axetil-loaded pH-responsive liposomes for arthritis treatment. *Chem. Eng. J.* **2024**, *482*, 148840. [CrossRef]

62. Abd-El-Azim, H.; Abbas, H.; El Sayed, N.S.; Fayez, A.M.; Zewail, M. Non-invasive management of rheumatoid arthritis using hollow microneedles as a tool for transdermal delivery of teriflunomide loaded solid lipid nanoparticles. *Int. J. Pharm.* **2023**, *644*, 123334. [CrossRef] [PubMed]

63. Kawre, S.; Suryavanshi, P.; Lalchandani, D.S.; Deka, M.K.; Porwal, P.K.; Kaity, S.; Roy, S.; Banerjee, S. Bioinspired labrum-shaped stereolithography (SLA) assisted 3D printed hollow microneedles (HMNs) for effectual delivery of ceftriaxone sodium. *Eur. Polym. J.* **2024**, *204*, 112702. [CrossRef]

64. Golombek, S.; Pilz, M.; Steinle, H.; Kochba, E.; Levin, Y.; Lunter, D.; Schlensak, C.; Wendel, H.P.; Avci-Adali, M. Intradermal Delivery of Synthetic mRNA Using Hollow Microneedles for Efficient and Rapid Production of Exogenous Proteins in Skin. *Mol. Ther. Nucleic Acids* **2018**, *11*, 382–392. [CrossRef] [PubMed]

65. van der Maaden, K.; Heuts, J.; Camps, M.; Pontier, M.; van Scheltinga, A.T.; Jiskoot, W.; Ossendorp, F.; Bouwstra, J. Hollow microneedle-mediated micro-injections of a liposomal HPV E743–63 synthetic long peptide vaccine for efficient induction of cytotoxic and T-helper responses. *J. Control. Release* **2018**, *269*, 347–354. [CrossRef] [PubMed]

66. Iliescu, F.S.; Teo, J.C.M.; Vrtacnik, D.; Taylor, H.; Iliescu, C. Cell therapy using an array of ultrathin hollow microneedles. *Microsyst. Technol.* **2018**, *24*, 2905–2912. [CrossRef]

67. Yin, S.; Yu, Z.; Song, N.; Guo, Z.; Li, W.; Ma, J.; Wang, X.; Liu, J.; Liang, M. A long lifetime and highly sensitive wearable microneedle sensor for the continuous real-time monitoring of glucose in interstitial fluid. *Biosens. Bioelectron.* **2024**, *244*, 115822. [CrossRef] [PubMed]

68. Drăgan, A.-M.; Parrilla, M.; Cambré, S.; Domínguez-Robles, J.; Detamornrat, U.; Donnelly, R.F.; Oprean, R.; Cristea, C.; De Wael, K. Microneedle array-based electrochemical sensor functionalized with SWCNTs for the highly sensitive monitoring of MDMA in interstitial fluid. *Microchem. J.* **2023**, *193*, 109257. [CrossRef]

69. Abbasiasl, T.; Mirlou, F.; Mirzajani, H.; Bathaei, M.J.; Istif, E.; Shomalizadeh, N.; Cebecioğlu, R.E.; Özkahraman, E.E.; Yener, U.C.; Beker, L. A Wearable Touch-Activated Device Integrated with Hollow Microneedles for Continuous Sampling and Sensing of Dermal Interstitial Fluid. *Adv. Mater.* **2024**, *36*, e2304704. [CrossRef]

70. Aziz, A.Y.R.; Hasir, N.A.; Imran, N.B.P.; Hamdan, M.F.; Mahfufah, U.; Wafiah, N.; Arjuna, A.; Utami, R.N.; Permana, A.D. Development of hydrogel-forming microneedles for transdermal delivery of albendazole from liquid reservoir. *J. Biomater. Sci. Polym. Ed.* **2023**, *34*, 1101–1120. [CrossRef]

71. Elim, D.; Fitri, A.M.N.; Mahfud, M.A.S.; Afika, N.; Sultan, N.A.F.; Hijrah; Asri, R.M.; Permana, A.D. Hydrogel forming microneedle-mediated transdermal delivery of sildenafil citrate from polyethylene glycol reservoir: An ex vivo proof of concept study. *Colloids Surf. B Biointerfaces* **2023**, *222*, 113018. [CrossRef] [PubMed]

72. Migdadi, E.M.; Courtenay, A.J.; Tekko, I.A.; McCrudden, M.T.; Kearney, M.-C.; McAlister, E.; McCarthy, H.O.; Donnelly, R.F. Hydrogel-forming microneedles enhance transdermal delivery of metformin hydrochloride. *J. Control. Release* **2018**, *285*, 142–151. [CrossRef] [PubMed]

73. Sivaraman, A.; Banga, A.K. Novel in situ forming hydrogel microneedles for transdermal drug delivery. *Drug Deliv. Transl. Res.* **2017**, *7*, 16–26. [CrossRef] [PubMed]

74. Anjani, Q.K.; Permana, A.D.; Cárcamo-Martínez, Á.; Domínguez-Robles, J.; Tekko, I.A.; Larrañeta, E.; Vora, L.K.; Ramadon, D.; Donnelly, R.F. Versatility of hydrogel-forming microneedles in in vitro transdermal delivery of tuberculosis drugs. *Eur. J. Pharm. Biopharm.* **2021**, *158*, 294–312. [CrossRef] [PubMed]

75. Leanpolchareanchai, J.; Nuchtavorn, N. Response Surface Methodology for Optimization of Hydrogel-Forming Microneedles as Rapid and Efficient Transdermal Microsampling Tools. *Gels* **2023**, *9*, 306. [CrossRef]

76. Mikszta, J.A.; Alarcon, J.B.; Brittingham, J.M.; Sutter, D.E.; Pettis, R.J.; Harvey, N.G. Improved genetic immunization via micromechanical disruption of skin-barrier function and targeted epidermal delivery. *Nat. Med.* **2002**, *8*, 415–419. [CrossRef] [PubMed]

77. Sabri, A.; Ogilvie, J.; McKenna, J.; Segal, J.; Scurr, D.; Marlow, M. Intradermal Delivery of an Immunomodulator for Basal Cell Carcinoma; Expanding the Mechanistic Insight into Solid Microneedle-Enhanced Delivery of Hydrophobic Molecules. *Mol. Pharm.* **2020**, *17*, 2925–2937. [CrossRef] [PubMed]

78. Elahpour, N.; Pahlevanzadeh, F.; Kharaziha, M.; Bakhsheshi-Rad, H.R.; Ramakrishna, S.; Berto, F. 3D printed microneedles for transdermal drug delivery: A brief review of two decades. *Int. J. Pharm.* **2021**, *597*, 120301. [CrossRef] [PubMed]

79. Larrañeta, E.; Lutton, R.E.M.; Woolfson, A.D.; Donnelly, R.F. Microneedle arrays as transdermal and intradermal drug delivery systems: Materials science, manufacture and commercial development. *Mater. Sci. Eng. R Rep.* **2016**, *104*, 1–32. [CrossRef]

80. Donnelly, R.F.; Singh, T.R.R.; Alkilani, A.Z.; McCrudden, M.T.C.; O'Neill, S.; O'Mahony, C.; Armstrong, K.; McLoone, N.; Kole, P.; Woolfson, A.D. Hydrogel-forming microneedle arrays exhibit antimicrobial properties: Potential for enhanced patient safety. *Int. J. Pharm.* **2013**, *451*, 76–91. [CrossRef]

81. Parhi, R. A review of three-dimensional printing for pharmaceutical applications: Quality control, risk assessment and future perspectives. *J. Drug Deliv. Sci. Technol.* **2021**, *64*, 102571. [CrossRef]

82. Gupta, J.; Gill, H.S.; Andrews, S.N.; Prausnitz, M.R. Kinetics of skin resealing after insertion of microneedles in human subjects. *J. Control. Release* **2011**, *154*, 148–155. [CrossRef]

83. Chen, Y.; Chen, B.Z.; Wang, Q.L.; Jin, X.; Guo, X.D. Fabrication of coated polymer microneedles for transdermal drug delivery. *J. Control. Release* **2017**, *265*, 14–21. [CrossRef]

84. Ingrole, R.S.; Gill, H.S. Microneedle Coating Methods: A Review with a Perspective. *J. Pharmacol. Exp. Ther.* **2019**, *370*, 555–569. [CrossRef]

85. Vrdoljak, A.; McGrath, M.G.; Carey, J.B.; Draper, S.J.; Hill, A.V.; O'Mahony, C.; Crean, A.M.; Moore, A.C. Coated microneedle arrays for transcutaneous delivery of live virus vaccines. *J. Control. Release* **2012**, *159*, 34–42. [CrossRef] [PubMed]

86. Chong, R.H.; Gonzalez-Gonzalez, E.; Lara, M.F.; Speaker, T.J.; Contag, C.H.; Kaspar, R.L.; Coulman, S.A.; Hargest, R.; Birchall, J.C. Gene silencing following siRNA delivery to skin via coated steel microneedles: In vitro and in vivo proof-of-concept. *J. Control. Release* **2013**, *166*, 211–219. [CrossRef]

87. Choi, H.-J.; Yoo, D.-G.; Bondy, B.J.; Quan, F.-S.; Compans, R.W.; Kang, S.-M.; Prausnitz, M.R. Stability of influenza vaccine coated onto microneedles. *Biomaterials* **2012**, *33*, 3756–3769. [CrossRef] [PubMed]

88. Pere, C.P.P.; Economidou, S.N.; Lall, G.; Ziraud, C.; Boateng, J.S.; Alexander, B.D.; Lamprou, D.A.; Douroumis, D. 3D printed microneedles for insulin skin delivery. *Int. J. Pharm.* **2018**, *544*, 425–432. [CrossRef]

89. Li, J.; Zeng, M.; Shan, H.; Tong, C. Microneedle Patches as Drug and Vaccine Delivery Platform. *Curr. Med. Chem.* **2017**, *24*, 2413–2422. [CrossRef] [PubMed]

90. Makvandi, P.; Maleki, A.; Shabani, M.; Hutton, A.R.; Kirkby, M.; Jamaledin, R.; Fang, T.; He, J.; Lee, J.; Mazzolai, B.; et al. Bioinspired microneedle patches: Biomimetic designs, fabrication, and biomedical applications. *Matter* **2022**, *5*, 390–429. [CrossRef]

91. Park, J.-H.; Allen, M.G.; Prausnitz, M.R. Polymer Microneedles for Controlled-Release Drug Delivery. *Pharm. Res.* **2006**, *23*, 1008–1019. [CrossRef]

92. McCrudden, M.T.; Alkilani, A.Z.; McCrudden, C.M.; McAlister, E.; McCarthy, H.O.; Woolfson, A.D.; Donnelly, R.F. Design and physicochemical characterisation of novel dissolving polymeric microneedle arrays for transdermal delivery of high dose, low molecular weight drugs. *J. Control. Release* **2014**, *180*, 71–80. [CrossRef]

93. Long, L.; Ji, D.; Hu, C.; Yang, L.; Tang, S.; Wang, Y. Microneedles for in situ tissue regeneration. *Mater. Today Bio* **2023**, *19*, 100579. [CrossRef]

94. Bauleth-Ramos, T.; El-Sayed, N.; Fontana, F.; Lobita, M.; Shahbazi, M.-A.; Santos, H.A. Recent approaches for enhancing the performance of dissolving microneedles in drug delivery applications. *Mater. Today* **2023**, *63*, 239–287. [CrossRef]

95. Lee, K.; Jung, H. Drawing lithography for microneedles: A review of fundamentals and biomedical applications. *Biomaterials* **2012**, *33*, 7309–7326. [CrossRef]

96. Lee, K.; Lee, C.Y.; Jung, H. Dissolving microneedles for transdermal drug administration prepared by stepwise controlled drawing of maltose. *Biomaterials* **2011**, *32*, 3134–3140. [CrossRef]

97. Miyano, T.; Tobinaga, Y.; Kanno, T.; Matsuzaki, Y.; Takeda, H.; Wakui, M.; Hanada, K. Sugar Micro Needles as Transdermic Drug Delivery System. *Biomed. Microdevices* **2005**, *7*, 185–188. [CrossRef] [PubMed]

98. Li, G.; Badkar, A.; Nema, S.; Kolli, C.S.; Banga, A.K. In vitro transdermal delivery of therapeutic antibodies using maltose microneedles. *Int. J. Pharm.* **2009**, *368*, 109–115. [CrossRef]

99. Yang, B.; Dong, Y.; Shen, Y.; Hou, A.; Quan, G.; Pan, X.; Wu, C. Bilayer dissolving microneedle array containing 5-fluorouracil and triamcinolone with biphasic release profile for hypertrophic scar therapy. *Bioact. Mater.* **2021**, *6*, 2400–2411. [CrossRef] [PubMed]

100. Choi, S.Y.; Kwon, H.J.; Ahn, G.R.; Ko, E.J.; Yoo, K.H.; Kim, B.J.; Lee, C.; Kim, D. Hyaluronic acid microneedle patch for the improvement of crow's feet wrinkles. *Dermatol. Ther.* **2017**, *30*, e12546. [CrossRef] [PubMed]

101. Park, Y.; Kim, B. Skin permeability of compounds loaded within dissolving microneedles dependent on composition of sodium hyaluronate and carboxymethyl cellulose. *Korean J. Chem. Eng.* **2017**, *34*, 133–138. [CrossRef]

102. Zvezdin, V.; Kasatkina, T.; Kasatkin, I.; Gavrilova, M.; Kazakova, O. Microneedle patch based on dissolving, detachable microneedle technology for improved skin quality of the periorbital region. Part 2: Clinical Evaluation. *Int. J. Cosmet. Sci.* **2020**, *42*, 429–435. [CrossRef]

103. Yalcintas, E.P.; Ackerman, D.S.; Korkmaz, E.; Telmer, C.A.; Jarvik, J.W.; Campbell, P.G.; Bruchez, M.P.; Ozdoganlar, O.B. Analysis of In Vitro Cytotoxicity of Carbohydrate-Based Materials Used for Dissolvable Microneedle Arrays. *Pharm. Res.* **2020**, *37*, 1–18. [CrossRef]

104. Reineccius, G. 9-Controlled release of flavour in food products. In *Modifying Flavour in Food*; Taylor, A., Hort, J., Eds.; Woodhead Publishing Series in Food Science, Technology and Nutrition; Woodhead Publishing: Sawston, Cambridge, 2007; pp. 169–184. [CrossRef]

105. Lee, B.-M.; Lee, C.; Lahiji, S.F.; Jung, U.-W.; Chung, G.; Jung, H. Dissolving Microneedles for Rapid and Painless Local Anesthesia. *Pharmaceutics* **2020**, *12*, 366. [CrossRef] [PubMed]

106. Ono, A.; Ito, S.; Sakagami, S.; Asada, H.; Saito, M.; Quan, Y.-S.; Kamiyama, F.; Hirobe, S.; Okada, N. Development of Novel Faster-Dissolving Microneedle Patches for Transcutaneous Vaccine Delivery. *Pharmaceutics* **2017**, *9*, 27. [CrossRef] [PubMed]

107. Huang, Y.; Yu, H.; Wang, L.; Shen, D.; Ni, Z.; Ren, S.; Lu, Y.; Chen, X.; Yang, J.; Hong, Y. Research progress on cosmetic microneedle systems: Preparation, property and application. *Eur. Polym. J.* **2022**, *163*, 110942. [CrossRef]

108. Ke, C.-L.; Deng, F.-S.; Chuang, C.-Y.; Lin, C.-H. Antimicrobial Actions and Applications of Chitosan. *Polymers* **2021**, *13*, 904. [CrossRef] [PubMed]

109. Chen, M.-C.; Huang, S.-F.; Lai, K.-Y.; Ling, M.-H. Fully embeddable chitosan microneedles as a sustained release depot for intradermal vaccination. *Biomaterials* **2013**, *34*, 3077–3086. [CrossRef]

110. Chiu, Y.-H.; Chen, M.-C.; Wan, S.-W. Sodium Hyaluronate/Chitosan Composite Microneedles as a Single-Dose Intradermal Immunization System. *Biomacromolecules* **2018**, *19*, 2278–2285. [CrossRef]

111. Kean, T.; Thanou, M. Biodegradation, biodistribution and toxicity of chitosan. *Adv. Drug Deliv. Rev.* **2010**, *62*, 3–11. [CrossRef]

112. Zhang, L.; Guo, R.; Wang, S.; Yang, X.; Ling, G.; Zhang, P. Fabrication, evaluation and applications of dissolving microneedles. *Int. J. Pharm.* **2021**, *604*, 120749. [CrossRef] [PubMed]

113. Fonseca, D.F.S.; Vilela, C.; Silvestre, A.J.D.; Freire, C.S.R. A compendium of current developments on polysaccharide and protein-based microneedles. *Int. J. Biol. Macromol.* **2019**, *136*, 704–728. [CrossRef] [PubMed]

114. Désévaux, C.; Dubreuil, P.; Lenaerts, V.; Girard, C. Tissue reaction and biodegradation of implanted cross-linked high amylose starch in rats. *J. Biomed. Mater. Res.* **2002**, *63*, 772–779. [CrossRef] [PubMed]

115. Cao, Y.; Wang, B. Biodegradation of Silk Biomaterials. *Int. J. Mol. Sci.* **2009**, *10*, 1514–1524. [CrossRef]

116. Wang, S.; Zhu, M.; Zhao, L.; Kuang, D.; Kundu, S.C.; Lu, S. Insulin-Loaded Silk Fibroin Microneedles as Sustained Release System. *ACS Biomater. Sci. Eng.* **2019**, *5*, 1887–1894. [CrossRef] [PubMed]

117. Lee, J.; Park, S.H.; Seo, I.H.; Lee, K.J.; Ryu, W. Rapid and repeatable fabrication of high A/R silk fibroin microneedles using thermally-drawn micromolds. *Eur. J. Pharm. Biopharm.* **2015**, *94*, 11–19. [CrossRef]

118. Zhu, M.; Liu, Y.; Jiang, F.; Cao, J.; Lu, S. Combined Silk Fibroin Microneedles for Insulin Delivery. *ACS Biomater. Sci. Eng.* **2020**, *6*, 3422–3429. [CrossRef] [PubMed]

119. Tsioris, K.; Raja, W.K.; Pritchard, E.M.; Panilaitis, B.; Kaplan, D.L.; Omenetto, F.G. Fabrication of Silk Microneedles for Controlled-Release Drug Delivery. *Adv. Funct. Mater.* **2012**, *22*, 330–335. [CrossRef]

120. Stinson, J.A.; Raja, W.K.; Lee, S.; Kim, H.B.; Diwan, I.; Tutunjian, S.; Panilaitis, B.; Omenetto, F.G.; Tzipori, S.; Kaplan, D.L. Silk Fibroin Microneedles for Transdermal Vaccine Delivery. *ACS Biomater. Sci. Eng.* **2017**, *3*, 360–369. [CrossRef]

121. Mao, J.; Wang, H.; Xie, Y.; Fu, Y.; Li, Y.; Liu, P.; Du, H.; Zhu, J.; Dong, L.; Hussain, M.; et al. Transdermal delivery of rapamycin with poor water-solubility by dissolving polymeric microneedles for anti-angiogenesis. *J. Mater. Chem. B* **2020**, *8*, 928–934. [CrossRef]

122. Yu, K.; Yu, X.; Cao, S.; Wang, Y.; Zhai, Y.; Yang, F.; Yang, X.; Lu, Y.; Wu, C.; Xu, Y. Layered dissolving microneedles as a need-based delivery system to simultaneously alleviate skin and joint lesions in psoriatic arthritis. *Acta Pharm. Sin. B* **2021**, *11*, 505–519. [CrossRef] [PubMed]

123. Vicente-Perez, E.M.; Larrañeta, E.; McCrudden, M.T.C.; Kissenpfennig, A.; Hegarty, S.; McCarthy, H.O.; Donnelly, R.F. Repeat application of microneedles does not alter skin appearance or barrier function and causes no measurable disturbance of serum biomarkers of infection, inflammation or immunity in mice in vivo. *Eur. J. Pharm. Biopharm.* **2017**, *117*, 400–407. [CrossRef] [PubMed]

124. Shim, W.S.; Hwang, Y.M.; Park, S.G.; Lee, C.K.; Kang, N.G. Role of Polyvinylpyrrolidone in Dissolving Microneedle for Efficient Transdermal Drug Delivery: In vitro and Clinical Studies. *Bull. Korean Chem. Soc.* **2018**, *39*, 789–793. [CrossRef]

125. EFSA Panel on Food Additives and Flavourings (FAF); Younes, M.; Aquilina, G.; Castle, L.; Engel, K.; Fowler, P.; Fürst, P.; Gürtler, R.; Gundert-Remy, U.; Husøy, T.; et al. Re-evaluation of polyvinylpyrrolidone (E 1201) and polyvinylpolypyrrolidone (E 1202) as food additives and extension of use of polyvinylpyrrolidone (E 1201). *EFSA J.* **2020**, *18*, e06215. [CrossRef] [PubMed]

126. Chen, B.Z.; Ashfaq, M.; Zhang, X.P.; Zhang, J.N.; Guo, X.D. In vitro and in vivo assessment of polymer microneedles for controlled transdermal drug delivery. *J. Drug Target.* **2018**, *26*, 720–729. [CrossRef] [PubMed]

127. Zhang, X.P.; Wang, B.B.; Li, W.X.; Fei, W.M.; Cui, Y.; Guo, X.D. In vivo safety assessment, biodistribution and toxicology of polyvinyl alcohol microneedles with 160-day uninterruptedly applications in mice. *Eur. J. Pharm. Biopharm.* **2021**, *160*, 1–8. [CrossRef]

128. Arya, J.; Henry, S.; Kalluri, H.; McAllister, D.V.; Pewin, W.P.; Prausnitz, M.R. Tolerability, usability and acceptability of dissolving microneedle patch administration in human subjects. *Biomaterials* **2017**, *128*, 1–7. [CrossRef]

129. Schmidt, S.J.; Holt, B.D.; Arnold, A.M.; Sydlik, S.A. Polyester functional graphenic materials as a mechanically enhanced scaffold for tissue regeneration. *RSC Adv.* **2020**, *10*, 8548–8557. [CrossRef]

130. Zhang, J.; Wang, Y.; Jin, J.Y.; Degan, S.; Hall, R.P.; Boehm, R.D.; Jaipan, P.; Narayan, R.J. Use of Drawing Lithography-Fabricated Polyglycolic Acid Microneedles for Transdermal Delivery of Itraconazole to a Human Basal Cell Carcinoma Model Regenerated on Mice. *JOM* **2016**, *68*, 1128–1133. [CrossRef]

131. Li, W.; Tang, J.; Terry, R.N.; Li, S.; Brunie, A.; Callahan, R.L.; Noel, R.K.; Rodríguez, C.A.; Schwendeman, S.P.; Prausnitz, M.R. Long-acting reversible contraception by effervescent microneedle patch. *Sci. Adv.* **2023**, *5*, eaaw8145. [CrossRef]

132. Tran, K.T.M.; Gavitt, T.D.; Farrell, N.J.; Curry, E.J.; Mara, A.B.; Patel, A.; Brown, L.; Kilpatrick, S.; Piotrowska, R.; Mishra, N.; et al. Transdermal microneedles for the programmable burst release of multiple vaccine payloads. *Nat. Biomed. Eng.* **2021**, *5*, 998–1007. [CrossRef]

133. Eum, J.; Kim, Y.; Um, D.J.; Shin, J.; Yang, H.; Jung, H. Solvent-Free Polycaprolactone Dissolving Microneedles Generated via the Thermal Melting Method for the Sustained Release of Capsaicin. *Micromachines* **2021**, *12*, 167. [CrossRef]

134. Sonetha, V.; Majumdar, S.; Shah, S. Step-wise micro-fabrication techniques of microneedle arrays with applications in transdermal drug delivery—A review. *J. Drug Deliv. Sci. Technol.* **2022**, *68*, 103119. [CrossRef]

135. Zhao, L.; Mu, J.; Du, P.; Wang, H.; Mao, Y.; Xu, Y.; Xin, X.; Zang, F. Ultrasound-guided core needle biopsy in the diagnosis of neuroblastic tumors in children: A retrospective study on 83 cases. *Pediatr. Surg. Int.* **2017**, *33*, 347–353. [CrossRef]

136. Yang, D.; Chen, M.; Sun, Y.; Jin, Y.; Lu, C.; Pan, X.; Quan, G.; Wu, C. Microneedle-mediated transdermal drug delivery for treating diverse skin diseases. *Acta Biomater.* **2021**, *121*, 119–133. [CrossRef]

137. Sharma, S.; Hatware, K.; Bhadane, P.; Sindhikar, S.; Mishra, D.K. Recent advances in microneedle composites for biomedical applications: Advanced drug delivery technologies. *Mater. Sci. Eng. C* **2019**, *103*, 109717. [CrossRef]

138. Turner, J.G.; White, L.R.; Estrela, P.; Leese, H.S. Hydrogel-Forming Microneedles: Current Advancements and Future Trends. *Macromol. Biosci.* **2021**, *21*, e2000307. [CrossRef] [PubMed]

139. Aung, N.N.; Ngawhirunpat, T.; Rojanarata, T.; Patrojanasophon, P.; Pamornpathomkul, B.; Opanasopit, P. Fabrication, characterization and comparison of α-arbutin loaded dissolving and hydrogel forming microneedles. *Int. J. Pharm.* **2020**, *586*, 119508. [CrossRef]

140. Lee, K.J.; Jeong, S.S.; Roh, D.H.; Kim, D.Y.; Choi, H.-K.; Lee, E.H. A practical guide to the development of microneedle systems—In clinical trials or on the market. *Int. J. Pharm.* **2020**, *573*, 118778. [CrossRef] [PubMed]

141. Le, Z.; Yu, J.; Quek, Y.J.; Bai, B.; Li, X.; Shou, Y.; Myint, B.; Xu, C.; Tay, A. Design principles of microneedles for drug delivery and sampling applications. *Mater. Today* **2023**, *63*, 137–169. [CrossRef]

142. Prausnitz, M.R.; Langer, R. Transdermal drug delivery. *Nat. Biotechnol.* **2008**, *26*, 1261–1268. [CrossRef] [PubMed]

143. Holbrook, K.A.; Odland, G.F. Regional Differences in the Thickness (Cell Layers) of the Human Stratum Corneum: An Ultrastructural Analysis. *J. Investig. Dermatol.* **1974**, *62*, 415–422. [CrossRef] [PubMed]

144. Planz, V.; Lehr, C.-M.; Windbergs, M. In vitro models for evaluating safety and efficacy of novel technologies for skin drug delivery. *J. Control. Release* **2016**, *242*, 89–104. [CrossRef] [PubMed]

145. Verbaan, F.J.; Bal, S.M.; Van den Berg, D.J.; Groenink, W.H.H.; Verpoorten, H.; Lüttge, R.; Bouwstra, J.A. Assembled microneedle arrays enhance the transport of compounds varying over a large range of molecular weight across human dermatomed skin. *J. Control. Release* **2007**, *117*, 238–245. [CrossRef] [PubMed]

146. Donnelly, R.F.; Garland, M.J.; Morrow, D.I.; Migalska, K.; Singh, T.R.R.; Majithiya, R.; Woolfson, A.D. Optical coherence tomography is a valuable tool in the study of the effects of microneedle geometry on skin penetration characteristics and in-skin dissolution. *J. Control. Release* **2010**, *147*, 333–341. [CrossRef]

147. Davidson, A.; Al-Qallaf, B.; Das, D.B. Transdermal drug delivery by coated microneedles: Geometry effects on effective skin thickness and drug permeability. *Chem. Eng. Res. Des.* **2008**, *86*, 1196–1206. [CrossRef]

148. Badran, M.; Kuntsche, J.; Fahr, A. Skin penetration enhancement by a microneedle device (Dermaroller®) in vitro: Dependency on needle size and applied formulation. *Eur. J. Pharm. Sci.* **2009**, *36*, 511–523. [CrossRef] [PubMed]

149. Xiu, X.; Gao, G.; Liu, Y.; Ma, F. Drug delivery with dissolving microneedles: Skin puncture, its influencing factors and improvement strategies. *J. Drug Deliv. Sci. Technol.* **2022**, *76*, 103653. [CrossRef]

150. Gill, H.S.; Denson, D.D.; Burris, B.A.B.; Prausnitz, M.R. Effect of Microneedle Design on Pain in Human Volunteers. *Clin. J. Pain* **2008**, *24*, 585–594. [CrossRef]

151. Kochhar, J.S.; Quek, T.C.; Soon, W.J.; Choi, J.; Zou, S.; Kang, L. Effect of Microneedle Geometry and Supporting Substrate on Microneedle Array Penetration into Skin. *J. Pharm. Sci.* **2013**, *102*, 4100–4108. [CrossRef]

152. Olatunji, O.; Das, D.B.; Garland, M.J.; Belaid, L.; Donnelly, R.F. Influence of Array Interspacing on the Force Required for Successful Microneedle Skin Penetration: Theoretical and Practical Approaches. *J. Pharm. Sci.* **2013**, *102*, 1209–1221. [CrossRef]

153. Prausnitz, M.R. Microneedles for transdermal drug delivery. *Adv. Drug Deliv. Rev.* **2004**, *56*, 581–587. [CrossRef] [PubMed]

154. Davis, S.P.; Landis, B.J.; Adams, Z.H.; Allen, M.G.; Prausnitz, M.R. Insertion of microneedles into skin: Measurement and prediction of insertion force and needle fracture force. *J. Biomech.* **2004**, *37*, 1155–1163. [CrossRef] [PubMed]

155. Bal, S.M.; Kruithof, A.C.; Zwier, R.; Dietz, E.; Bouwstra, J.A.; Lademann, J.; Meinke, M.C. Influence of microneedle shape on the transport of a fluorescent dye into human skin in vivo. *J. Control. Release* **2010**, *147*, 218–224. [CrossRef]

156. Park, J.-H.; Yoon, Y.-K.; Choi, S.-O.; Prausnitz, M.R.; Allen, M.G. Tapered Conical Polymer Microneedles Fabricated Using an Integrated Lens Technique for Transdermal Drug Delivery. *IEEE Trans. Biomed. Eng.* **2007**, *54*, 903–913. [CrossRef]

157. Römgens, A.; Bader, D.; Bouwstra, J.; Baaijens, F.; Oomens, C. Monitoring the penetration process of single microneedles with varying tip diameters. *J. Mech. Behav. Biomed. Mater.* **2014**, *40*, 397–405. [CrossRef]

158. Sabri, A.H.; Kim, Y.; Marlow, M.; Scurr, D.J.; Segal, J.; Banga, A.K.; Kagan, L.; Lee, J.B. Intradermal and transdermal drug delivery using microneedles—Fabrication, performance evaluation and application to lymphatic delivery. *Adv. Drug Deliv. Rev.* **2020**, *153*, 195–215. [CrossRef]

159. Bao, L.; Park, J.; Bonfante, G.; Kim, B. Recent advances in porous microneedles: Materials, fabrication, and transdermal applications. *Drug Deliv. Transl. Res.* **2022**, *12*, 395–414. [CrossRef]

160. Park, J.-H.; Prausnitz, M. Analysis of mechanical failure of polymer microneedles by axial force. *J. Korean Phys. Soc.* **2010**, *56*, 1223–1227. [CrossRef]

161. Chang, K.-T.; Shen, Y.-K.; Fan, F.-Y.; Lin, Y.; Kang, S.-C. Optimal design and fabrication of a microneedle arrays patch. *J. Manuf. Process.* **2020**, *54*, 274–285. [CrossRef]

162. Gittard, S.D.; Chen, B.; Xu, H.; Ovsianikov, A.; Chichkov, B.N.; Monteiro-Riviere, N.A.; Narayan, R.J. The effects of geometry on skin penetration and failure of polymer microneedles. *J. Adhes. Sci. Technol.* **2013**, *27*, 227–243. [CrossRef] [PubMed]

163. Li, Y.; Hu, X.; Dong, Z.; Chen, Y.; Zhao, W.; Wang, Y.; Zhang, L.; Chen, M.; Wu, C.; Wang, Q. Dissolving Microneedle Arrays with Optimized Needle Geometry for Transcutaneous Immunization. *Eur. J. Pharm. Sci.* **2020**, *151*, 105361. [CrossRef] [PubMed]

164. Loizidou, E.Z.; Inoue, N.T.; Ashton-Barnett, J.; Barrow, D.A.; Allender, C.J. Evaluation of geometrical effects of microneedles on skin penetration by CT scan and finite element analysis. *Eur. J. Pharm. Biopharm.* **2016**, *107*, 1–6. [CrossRef] [PubMed]

165. Lyu, S.; Dong, Z.; Xu, X.; Bei, H.-P.; Yuen, H.-Y.; Cheung, C.-W.J.; Wong, M.-S.; He, Y.; Zhao, X. Going below and beyond the surface: Microneedle structure, materials, drugs, fabrication, and applications for wound healing and tissue regeneration. *Bioact. Mater.* **2023**, *27*, 303–326. [CrossRef] [PubMed]

166. Aldawood, F.K.; Andar, A.; Desai, S. A Comprehensive Review of Microneedles: Types, Materials, Processes, Characterizations and Applications. *Polymers* **2021**, *13*, 2815. [CrossRef] [PubMed]

167. Bariya, S.H.; Gohel, M.C.; Mehta, T.A.; Sharma, O.P. Microneedles: An emerging transdermal drug delivery system. *J. Pharm. Pharmacol.* **2012**, *64*, 11–29. [CrossRef]

168. Tucak, A.; Sirbubalo, M.; Hindija, L.; Rahić, O.; Hadžiabdić, J.; Muhamedagić, K.; Čekić, A.; Vranić, E. Microneedles: Characteristics, Materials, Production Methods and Commercial Development. *Micromachines* **2020**, *11*, 961. [CrossRef]

169. Razali, A.R.; Qin, Y. A Review on Micro-manufacturing, Micro-forming and their Key Issues. *Procedia Eng.* **2013**, *53*, 665–672. [CrossRef]

170. Nuxoll, E. BioMEMS in drug delivery. *Adv. Drug Deliv. Rev.* **2013**, *65*, 1611–1625. [CrossRef]

171. Kathuria, H.; Kang, K.; Cai, J.; Kang, L. Rapid microneedle fabrication by heating and photolithography. *Int. J. Pharm.* **2020**, *575*, 118992. [CrossRef]

172. Pérennès, F.; Marmiroli, B.; Matteucci, M.; Tormen, M.; Vaccari, L.; Di Fabrizio, E. Sharp beveled tip hollow microneedle arrays fabricated by LIGA and 3D soft lithography with polyvinyl alcohol. *J. Micromech. Microeng.* **2006**, *16*, 473–479. [CrossRef]

173. Madou, M. *Fundamentals Of Microfabrication and Nanotechnology*, 1st ed.; CRC Press: Boca Raton, FL, USA, 2018.

174. Chaudhri, B.P.; Ceyssens, F.; Guan, T.; La Manna, A.; Neves, H.P.; Van Hoof, C.; Puers, R. High Strength, Polymer Microneedles for Transdermal Drug Delivery. *Procedia Eng.* **2011**, *25*, 1377–1380. [CrossRef]

175. Moon, S.J.; Lee, S.S.; Lee, H.S.; Kwon, T.H. Fabrication of microneedle array using LIGA and hot embossing process. *Microsyst. Technol.* **2005**, *11*, 311–318. [CrossRef]

176. Takahashi, H.; Heo, Y.J.; Arakawa, N.; Kan, T.; Matsumoto, K.; Kawano, R.; Shimoyama, I. Scalable fabrication of microneedle arrays via spatially controlled UV exposure. *Microsyst. Nanoeng.* **2016**, *2*, 16049. [CrossRef] [PubMed]

177. Takahashi, H.; Heo, Y.J.; Shimoyama, I. Scalable Fabrication of PEGDA Microneedles Using UV Exposure via a Rotating Prism. *J. Microelectromech. Syst.* **2017**, *26*, 990–992. [CrossRef]

178. Tomono, T. A new way to control the internal structure of microneedles: A case of chitosan lactate. *Mater. Today Chem.* **2019**, *13*, 79–87. [CrossRef]

179. Dharadhar, S.; Majumdar, A.; Dhoble, S.; Patravale, V. Microneedles for transdermal drug delivery: A systematic review. *Drug Dev. Ind. Pharm.* **2019**, *45*, 188–201. [CrossRef] [PubMed]

180. Donnelly, R.F.; Singh, T.R.R.; Tunney, M.M.; Morrow, D.I.J.; McCarron, P.A.; O'Mahony, C.; Woolfson, A.D. Microneedle Arrays Allow Lower Microbial Penetration Than Hypodermic Needles In Vitro. *Pharm. Res.* **2009**, *26*, 2513–2522. [CrossRef] [PubMed]

181. Li, Z.; Li, Y.; Liu, M.; Cui, L.; Yu, Y. Microneedle Electrode Array for Electrical Impedance Myography to Characterize Neurogenic Myopathy. *Ann. Biomed. Eng.* **2016**, *44*, 1566–1575. [CrossRef]

182. Li, Y.-C.; Feng, S.-J.; Chen, H.-X.; Chen, Z.-L.; Zhang, D.-M. Random vibration of train-track-ground system with a poroelastic interlayer in the subsoil. *Soil Dyn. Earthq. Eng.* **2019**, *120*, 1–11. [CrossRef]

183. Wilke, N.; Mulcahy, A.; Ye, S.-R.; Morrissey, A. Process optimization and characterization of silicon microneedles fabricated by wet etch technology. *Microelectron. J.* **2005**, *36*, 650–656. [CrossRef]

184. Liu, Y.; Eng, P.F.; Guy, O.J.; Roberts, K.; Ashraf, H.; Knight, N. Advanced deep reactive-ion etching technology for hollow microneedles for transdermal blood sampling and drug delivery. *IET Nanobiotechnol.* **2013**, *7*, 59–62. [CrossRef] [PubMed]

185. Roxhed, N.; Gasser, T.C.; Griss, P.; Holzapfel, G.A.; Stemme, G. Penetration-Enhanced Ultrasharp Microneedles and Prediction on Skin Interaction for Efficient Transdermal Drug Delivery. *J. Microelectromech. Syst.* **2007**, *16*, 1429–1440. [CrossRef]

186. Henry, S.; McAllister, D.V.; Allen, M.G.; Prausnitz, M.R. Microfabricated Microneedles: A Novel Approach to Transdermal Drug Delivery. *J. Pharm. Sci.* **1998**, *87*, 922–925. [CrossRef]

187. Wang, P.-C.; Wester, B.A.; Rajaraman, S.; Paik, S.-J.; Kim, S.-H.; Allen, M.G. Hollow polymer microneedle array fabricated by photolithography process combined with micromolding technique. In Proceedings of the 2009 Annual International Conference of the IEEE Engineering in Medicine and Biology Society, Minneapolis, MN, USA, 3–6 September 2009; pp. 7026–7029. [CrossRef]

188. Paik, S.-J.; Byun, S.; Lim, J.-M.; Park, Y.; Lee, A.; Chung, S.; Chang, J.; Chun, K.; Cho, D. In-plane single-crystal-silicon microneedles for minimally invasive microfluid systems. *Sens. Actuators A Phys.* **2004**, *114*, 276–284. [CrossRef]

189. Ma, B.; Liu, S.; Gan, Z.; Liu, G.; Cai, X.; Zhang, H.; Yang, Z. A PZT insulin pump integrated with a silicon microneedle array for transdermal drug delivery. *Microfluidics Nanofluidics* **2006**, *2*, 417–423. [CrossRef]

190. Wang, J.; Wang, H.; Lai, L.; Li, Y. Preparation of Microneedle Array Mold Based on MEMS Lithography Technology. *Micromachines* **2021**, *12*, 23. [CrossRef]

191. Chen, Z.; He, J.; Qi, J.; Zhu, Q.; Wu, W.; Lu, Y. Long-acting microneedles: A progress report of the state-of-the-art techniques. *Drug Discov. Today* **2020**, *25*, 1462–1468. [CrossRef]

192. Ita, K. Ceramic microneedles and hollow microneedles for transdermal drug delivery: Two decades of research. *J. Drug Deliv. Sci. Technol.* **2018**, *44*, 314–322. [CrossRef]

193. Chang, H.; Cui, Y. Image Classification Algorithm Based on Big Data and Multilabel Learning of Improved Convolutional Neural Network. *Wirel. Commun. Mob. Comput.* **2021**, *2021*, 3138398. [CrossRef]

194. Boks, M.A.; Unger, W.W.; Engels, S.; Ambrosini, M.; van Kooyk, Y.; Luttge, R. Controlled release of a model vaccine by nanoporous ceramic microneedle arrays. *Int. J. Pharm.* **2015**, *491*, 375–383. [CrossRef] [PubMed]

195. Bystrova, S.; Luttge, R. Micromolding for ceramic microneedle arrays. *Microelectron. Eng.* **2011**, *88*, 1681–1684. [CrossRef]

196. Yuan, W.; Yang, S.; Feng, Y.; Zhang, L.; Chen, N.; Jin, T. A scalable fabrication process of polymer microneedles. *Int. J. Nanomed.* **2012**, *7*, 1415–1422. [CrossRef] [PubMed]

197. Zhang, Y.; Jiang, G.; Yu, W.; Liu, D.; Xu, B. Microneedles fabricated from alginate and maltose for transdermal delivery of insulin on diabetic rats. *Mater. Sci. Eng. C* **2018**, *85*, 18–26. [CrossRef] [PubMed]

198. Park, J.-H.; Allen, M.G.; Prausnitz, M.R. Biodegradable polymer microneedles: Fabrication, mechanics and transdermal drug delivery. *J. Control. Release* **2005**, *104*, 51–66. [CrossRef] [PubMed]

199. Lee, J.; Kim, D.-H.; Lee, K.J.; Seo, I.H.; Park, S.H.; Jang, E.H.; Park, Y.; Youn, Y.-N.; Ryu, W. Transfer-molded wrappable microneedle meshes for perivascular drug delivery. *J. Control. Release* **2017**, *268*, 237–246. [CrossRef]

200. Moga, K.A.; Bickford, L.R.; Geil, R.D.; Dunn, S.S.; Pandya, A.A.; Wang, Y.; Fain, J.H.; Archuleta, C.F.; O'Neill, A.T.; DeSimone, J.M. Rapidly–Dissolvable Microneedle Patches Via a Highly Scalable and Reproducible Soft Lithography Approach. *Adv. Mater.* **2013**, *25*, 5060–5066. [CrossRef]

201. Lee, M.-T.; Lee, I.-C.; Tsai, S.-W.; Chen, C.-H.; Wu, M.-H.; Juang, Y.-J. Spin coating of polymer solution on polydimethylsiloxane mold for fabrication of microneedle patch. *J. Taiwan Inst. Chem. Eng.* **2017**, *70*, 42–48. [CrossRef]

202. McGrath, M.G.; Vucen, S.; Vrdoljak, A.; Kelly, A.; O'mahony, C.; Crean, A.M.; Moore, A. Production of dissolvable microneedles using an atomised spray process: Effect of microneedle composition on skin penetration. *Eur. J. Pharm. Biopharm.* **2014**, *86*, 200–211. [CrossRef]

203. Vrdoljak, A.; Allen, E.A.; Ferrara, F.; Temperton, N.J.; Crean, A.M.; Moore, A.C. Induction of broad immunity by thermostabilised vaccines incorporated in dissolvable microneedles using novel fabrication methods. *J. Control. Release* **2016**, *225*, 192–204. [CrossRef]

204. Kim, M.J.; Park, S.C.; Rizal, B.; Guanes, G.; Baek, S.-K.; Park, J.-H.; Betz, A.R.; Choi, S.-O. Fabrication of Circular Obelisk-Type Multilayer Microneedles Using Micro-Milling and Spray Deposition. *Front. Bioeng. Biotechnol.* **2018**, *6*, 54. [CrossRef] [PubMed]

205. Gill, H.S.; Prausnitz, M.R. Coated microneedles for transdermal delivery. *J. Control. Release* **2007**, *117*, 227–237. [CrossRef]

206. Martanto, W.; Davis, S.P.; Holiday, N.R.; Wang, J.; Gill, H.S.; Prausnitz, M.R. Transdermal Delivery of Insulin Using Microneedles in Vivo. *Pharm. Res.* **2004**, *21*, 947–952. [CrossRef] [PubMed]

207. Gill, H.S.; Prausnitz, M.R. Coating Formulations for Microneedles. *Pharm. Res.* **2007**, *24*, 1369–1380. [CrossRef]

208. Indermun, S.; Luttge, R.; Choonara, Y.E.; Kumar, P.; du Toit, L.C.; Modi, G.; Pillay, V. Current advances in the fabrication of microneedles for transdermal delivery. *J. Control. Release* **2014**, *185*, 130–138. [CrossRef]

209. Nagarkar, R.; Singh, M.; Nguyen, H.X.; Jonnalagadda, S. A review of recent advances in microneedle technology for transdermal drug delivery. *J. Drug Deliv. Sci. Technol.* **2020**, *59*, 101923. [CrossRef]

210. Omatsu, T.; Chujo, K.; Miyamoto, K.; Okida, M.; Nakamura, K.; Aoki, N.; Morita, R. Metal microneedle fabrication using twisted light with spin. *Opt. Express* **2010**, *18*, 17967–17973. [CrossRef]

211. Evens, T.; Malek, O.; Castagne, S.; Seveno, D.; Van Bael, A. A novel method for producing solid polymer microneedles using laser ablated moulds in an injection moulding process. *Manuf. Lett.* **2020**, *24*, 29–32. [CrossRef]

212. Aoyagi, S.; Izumi, H.; Isono, Y.; Fukuda, M.; Ogawa, H. Laser fabrication of high aspect ratio thin holes on biodegradable polymer and its application to a microneedle. *Sens. Actuators A Phys.* **2007**, *139*, 293–302. [CrossRef]

213. Albarahmieh, E.; AbuAmmouneh, L.; Kaddoura, Z.; AbuHantash, F.; Alkhalidi, B.A.; Al-Halhouli, A. Fabrication of Dissolvable Microneedle Patches Using an Innovative Laser-Cut Mould Design to Shortlist Potentially Transungual Delivery Systems: In Vitro Evaluation. *AAPS PharmSciTech* **2019**, *20*, 215. [CrossRef]

214. Nejad, H.R.; Sadeqi, A.; Kiaee, G.; Sonkusale, S. Low-cost and cleanroom-free fabrication of microneedles. *Microsyst. Nanoeng.* **2018**, *4*, 17073. [CrossRef]

215. Tu, K.T.; Chung, C.K. Rapid prototyping of biodegradable microneedle arrays by integrating $CO_2$ laser processing and polymer molding. *J. Micromech. Microeng.* **2016**, *26*, 65015. [CrossRef]

216. Demir, Y.K.; Akan, Z.; Kerimoglu, O. Characterization of Polymeric Microneedle Arrays for Transdermal Drug Delivery. *PLoS ONE* **2013**, *8*, e77289. [CrossRef]

217. Anbazhagan, G.; Suseela, S.B.; Sankararajan, R. Design, analysis and fabrication of solid polymer microneedle patch using $CO_2$ laser and polymer molding. *Drug Deliv. Transl. Res.* **2023**, *13*, 1813–1827. [CrossRef]

218. Adarkwa, E.; Desai, S. Scalable Droplet Based Manufacturing Using In-Flight Laser Evaporation. *J. Nanoeng. Nanomanuf.* **2016**, *6*, 87–92. [CrossRef]

219. Yang, M.; Xu, Z.; Desai, S.; Kumar, D.; Sankar, J. Fabrication of Micro Single Chamber Solid Oxide Fuel Cell Using Photolithography and Pulsed Laser Deposition. *J. Fuel Cell Sci. Technol.* **2015**, *12*, 021004. [CrossRef]

220. Esho, T.; Desai, S. Laser based microdroplet evaporation towards scalable micro and nano manufacturing. In Proceedings of the 62nd IIE Annual Conference and Expo, Orlando, FL, USA, 19–23 May 2012; pp. 1750–1757.

221. Parupelli, S.K.; Desai, S. Understanding Hybrid Additive Manufacturing of Functional Devices. *Am. J. Eng. Appl. Sci.* **2017**, *10*, 264–271. [CrossRef]

222. McKenzie, J.; Desai, S. Investigating Sintering Mechanisms for Additive Manufacturing of Conductive Traces. *Am. J. Eng. Appl. Sci.* **2018**, *11*, 652–662. [CrossRef]

223. Desai, S.; Craps, M.; Esho, T. Direct writing of nanomaterials for flexible thin-film transistors (fTFTs). *Int. J. Adv. Manuf. Technol.* **2013**, *64*, 537–543. [CrossRef]

224. Ahmed, M.; El-Naggar, M.E.; Aldalbahi, A.; El-Newehy, M.H.; Menazea, A. Methylene blue degradation under visible light of metallic nanoparticles scattered into graphene oxide using laser ablation technique in aqueous solutions. *J. Mol. Liq.* **2020**, *315*, 113794. [CrossRef]

225. Ismail, A.; El-Newehy, M.H.; El-Naggar, M.E.; Moydeen, A.M.; Menazea, A. Enhancement the electrical conductivity of the synthesized polyvinylidene fluoride/polyvinyl chloride composite doped with palladium nanoparticles via laser ablation. *J. Mater. Res. Technol.* **2020**, *9*, 11178–11188. [CrossRef]

226. Menazea, A.; El-Newehy, M.H.; Thamer, B.M.; El-Naggar, M.E. Preparation of antibacterial film-based biopolymer embedded with vanadium oxide nanoparticles using one-pot laser ablation. *J. Mol. Struct.* **2021**, *1225*, 129163. [CrossRef]

227. Tu, K.-T.; Chung, C.-K. Fabrication of biodegradable polymer microneedle array via $CO_2$ laser ablation. In Proceedings of the 2015 IEEE 10th International Conference on Nano/Micro Engineered and Molecular Systems (NEMS), Xi'an, China, 7–11 April 2015; pp. 494–497. [CrossRef]

228. Chen, Y.-T.; Ma, K.-J.; Tseng, A.A.; Chen, P. Projection ablation of glass-based single and arrayed microstructures using excimer laser. *Opt. Laser Technol.* **2005**, *37*, 271–280. [CrossRef]

229. Zheng, H.; Lam, Y.; Sundarraman, C.; Tran, D. Influence of substrate cooling on femtosecond laser machined hole depth and diameter. *Appl. Phys. A* **2007**, *89*, 559–563. [CrossRef]

230. Lutton, R.E.; Larrañeta, E.; Kearney, M.-C.; Boyd, P.; Woolfson, A.; Donnelly, R.F. A novel scalable manufacturing process for the production of hydrogel-forming microneedle arrays. *Int. J. Pharm.* **2015**, *494*, 417–429. [CrossRef] [PubMed]

231. Zaied, M.; Miraoui, I.; Boujelbene, M.; Bayraktar, E. Analysis of heat affected zone obtained by $CO_2$ laser cutting of low carbon steel (S235). In *AIP Conference Proceedings*; American Institute of Physics: College Park, MD, USA, 2013. [CrossRef]

232. Wang, Q.L.; Zhu, D.D.; Chen, Y.; Guo, X.D. A fabrication method of microneedle molds with controlled microstructures. *Mater. Sci. Eng. C* **2016**, *65*, 135–142. [CrossRef]

233. Chen, B.Z.; He, M.C.; Zhang, X.P.; Fei, W.M.; Cui, Y.; Guo, X.D. A novel method for fabrication of coated microneedles with homogeneous and controllable drug dosage for transdermal drug delivery. *Drug Deliv. Transl. Res.* **2022**, *12*, 2730–2739. [CrossRef] [PubMed]

234. Wang, P.M.; Cornwell, M.; Hill, J.; Prausnitz, M.R. Precise Microinjection into Skin Using Hollow Microneedles. *J. Investig. Dermatol.* **2006**, *126*, 1080–1087. [CrossRef] [PubMed]

235. Gupta, J.; Felner, E.I.; Prausnitz, M.R. Rapid Pharmacokinetics of Intradermal Insulin Administered Using Microneedles in Type 1 Diabetes Subjects. *Diabetes Technol. Ther.* **2011**, *13*, 451–456. [CrossRef]

236. Martanto, W.; Moore, J.S.; Kashlan, O.; Kamath, R.; Wang, P.M.; O'Neal, J.M.; Prausnitz, M.R. Microinfusion Using Hollow Microneedles. *Pharm. Res.* **2006**, *23*, 104–113. [CrossRef]

237. Mahadevan, G.; Sheardown, H.; Selvaganapathy, P. PDMS embedded microneedles as a controlled release system for the eye. *J. Biomater. Appl.* **2012**, *28*, 20–27. [CrossRef] [PubMed]

238. Kim, J.D.; Kim, M.; Yang, H.; Lee, K.; Jung, H. Droplet-born air blowing: Novel dissolving microneedle fabrication. *J. Control. Release* **2013**, *170*, 430–436. [CrossRef]

239. Wu, M.; Zhang, Y.; Huang, H.; Li, J.; Liu, H.; Guo, Z.; Xue, L.; Liu, S.; Lei, Y. Assisted 3D printing of microneedle patches for minimally invasive glucose control in diabetes. *Mater. Sci. Eng. C* **2020**, *117*, 111299. [CrossRef]

240. Kim, J.D.; Bae, J.-H.; Kim, H.K.; Jeong, D.H. Droplet-born Air Blowing (DAB) Technology for the Industrialization of Dissolving Microneedle. In Proceedings of the World Congress on Recent Advances in Nanotechnology, Prague, Czech Republic, 1–2 April 2016. [CrossRef]

241. Wu, L.; Takama, N.; Park, J.; Kim, B.; Kim, J.; Jeong, D. Shadow mask assisted droplet-born air-blowing method for fabrication of dissoluble microneedle. In Proceedings of the 2017 IEEE 12th International Conference on Nano/Micro Engineered and Molecular Systems (NEMS), Los Angeles, CA, USA, 9–12 April 2017; pp. 456–459.

242. Lin, Y.-H.; Lee, I.-C.; Hsu, W.-C.; Hsu, C.-H.; Chang, K.-P.; Gao, S.-S. Rapid fabrication method of a microneedle mold with controllable needle height and width. *Biomed. Microdevices* **2016**, *18*, 85. [CrossRef]

243. Vecchione, R.; Coppola, S.; Esposito, E.; Casale, C.; Vespini, V.; Grilli, S.; Ferraro, P.; Netti, P.A. Electro-Drawn Drug-Loaded Biodegradable Polymer Microneedles as a Viable Route to Hypodermic Injection. *Adv. Funct. Mater.* **2014**, *24*, 3515–3523. [CrossRef]

244. Lee, S.; Fakhraei Lahiji, S.; Jang, J.; Jang, M.; Jung, H. Micro-Pillar Integrated Dissolving Microneedles for Enhanced Transdermal Drug Delivery. *Pharmaceutics* **2019**, *11*, 402. [CrossRef] [PubMed]

245. Kim, M.J.; Park, S.C.; Choi, S.-O. Dual-nozzle spray deposition process for improving the stability of proteins in polymer microneedles. *RSC Adv.* **2017**, *7*, 55350–55359. [CrossRef]

246. Juster, H.; van der Aar, B.; de Brouwer, H. A review on microfabrication of thermoplastic polymer-based microneedle arrays. *Polym. Eng. Sci.* **2019**, *59*, 877–890. [CrossRef]

247. Lhernould, M.S.; Deleers, M.; Delchambre, A. Hollow polymer microneedles array resistance and insertion tests. *Int. J. Pharm.* **2015**, *480*, 152–157. [CrossRef]

248. Nair, K.J. Micro-Injection Molded Microneedles for Drug Delivery. Ph.D. Thesis, University of Bradford, Bradford, UK, 2016.

249. Sammoura, F.; Kang, J.; Heo, Y.-M.; Jung, T.; Lin, L. Polymeric microneedle fabrication using a microinjection molding technique. *Microsyst. Technol.* **2007**, *13*, 517–522. [CrossRef]

250. Bediz, B.; Korkmaz, E.; Khilwani, R.; Donahue, C.; Erdos, G.; Falo, L.D.; Ozdoganlar, O.B. Dissolvable Microneedle Arrays for Intradermal Delivery of Biologics: Fabrication and Application. *Pharm. Res.* **2014**, *31*, 117–135. [CrossRef] [PubMed]

251. Malek-Khatabi, A.; Rad, Z.F.; Rad-Malekshahi, M.; Akbarijavar, H. Development of dissolvable microneedle patches by CNC machining and micromolding for drug delivery. *Mater. Lett.* **2023**, *330*, 133328. [CrossRef]

252. García-López, E.; Siller, H.R.; Rodríguez, C.A. Study of the fabrication of AISI 316L microneedle arrays. *Procedia Manuf.* **2018**, *26*, 117–124. [CrossRef]

253. Parupelli, S.K.; Desai, S. A Comprehensive Review of Additive Manufacturing (3D Printing): Processes, Applications and Future Potential. *Am. J. Appl. Sci.* **2019**, *16*, 244–272. [CrossRef]

254. Adarkwa, E.; Kotoka, R.; Desai, S. 3D printing of polymeric Coatings on AZ31 Mg alloy Substrate for Corrosion Protection of biomedical implants. *Med. Devices Sens.* **2021**, *4*, e10167. [CrossRef]

255. Altubaishe, B.; Clarke, J.; McWilliams, C.; Desai, S. Comparative Analysis of Risk Management Strategies for Additive Manufacturing Supply Chains. *Am. J. Appl. Sci.* **2019**, *16*, 273–282. [CrossRef]

256. Aldawood, F.K.; Chang, S.X.; Desai, S. Design and manufacture of a high precision personalized electron bolus device for radiation therapy. *Med. Devices Sens.* **2020**, *3*, e10077. [CrossRef]

257. Haeberle, G.; Desai, S. Investigating Rapid Thermoform Tooling Via Additive Manufacturing (3D Printing). *Am. J. Appl. Sci.* **2019**, *16*, 238–243. [CrossRef]

258. Parupelli, S.K.; Desai, S. Hybrid additive manufacturing (3D printing) and characterization of functionally gradient materials via in situ laser curing. *Int. J. Adv. Manuf. Technol.* **2020**, *110*, 543–556. [CrossRef]

259. Economidou, S.N.; Lamprou, D.A.; Douroumis, D. 3D printing applications for transdermal drug delivery. *Int. J. Pharm.* **2018**, *544*, 415–424. [CrossRef]

260. Alhnan, M.A.; Okwuosa, T.C.; Sadia, M.; Wan, K.-W.; Ahmed, W.; Arafat, B. Emergence of 3D Printed Dosage Forms: Opportunities and Challenges. *Pharm. Res.* **2016**, *33*, 1817–1832. [CrossRef] [PubMed]

261. Jamróz, W.; Szafraniec, J.; Kurek, M.; Jachowicz, R. 3D Printing in Pharmaceutical and Medical Applications—Recent Achievements and Challenges. *Pharm. Res.* **2018**, *35*, 176. [CrossRef] [PubMed]

262. Prasad, L.K.; Smyth, H. 3D Printing technologies for drug delivery: A review. *Drug Dev. Ind. Pharm.* **2016**, *42*, 1019–1031. [CrossRef] [PubMed]

263. Lim, S.H.; Kathuria, H.; Tan, J.J.Y.; Kang, L. 3D printed drug delivery and testing systems—A passing fad or the future? *Adv. Drug Deliv. Rev.* **2018**, *132*, 139–168. [CrossRef] [PubMed]

264. Goole, J.; Amighi, K. 3D printing in pharmaceutics: A new tool for designing customized drug delivery systems. *Int. J. Pharm.* **2016**, *499*, 376–394. [CrossRef] [PubMed]

265. Awad, A.; Trenfield, S.J.; Gaisford, S.; Basit, A.W. 3D printed medicines: A new branch of digital healthcare. *Int. J. Pharm.* **2018**, *548*, 586–596. [CrossRef] [PubMed]

266. Camović, M.; Biščević, A.; Brčić, I.; Borčak, K.; Bušatlić, S.; Ćenanović, N.; Dedović, A.; Mulalić, A.; Osmanlić, M.; Sirbubalo, M.; et al. Coated 3D Printed PLA Microneedles as Transdermal Drug Delivery Systems. In Proceedings of the International Conference on Medical and Biological Engineering, Banja Luka, Bosnia and Herzegovina, 16–18 May 2019; Springer International Publishing: Berlin/Heidelberg, Germany, 2020; pp. 735–742. [CrossRef]

267. Luzuriaga, M.A.; Berry, D.R.; Reagan, J.C.; Smaldone, R.A.; Gassensmith, J.J. Biodegradable 3D printed polymer microneedles for transdermal drug delivery. *Lab Chip* **2018**, *18*, 1223–1230. [CrossRef] [PubMed]

268. Allen, E.A.; O'mahony, C.; Cronin, M.; O'mahony, T.; Moore, A.C.; Crean, A.M. Dissolvable microneedle fabrication using piezoelectric dispensing technology. *Int. J. Pharm.* **2016**, *500*, 1–10. [CrossRef] [PubMed]

269. Derakhshandeh, H.; Aghabaglou, F.; McCarthy, A.; Mostafavi, A.; Wiseman, C.; Bonick, Z.; Ghanavati, I.; Harris, S.; Kreikemeier-Bower, C.; Basri, S.M.M.; et al. A Wirelessly Controlled Smart Bandage with 3D-Printed Miniaturized Needle Arrays. *Adv. Funct. Mater.* **2020**, *30*, 1905544. [CrossRef]

270. Barnum, L.; Quint, J.; Derakhshandeh, H.; Samandari, M.; Aghabaglou, F.; Farzin, A.; Abbasi, L.; Bencherif, S.; Memic, A.; Mostafalu, P.; et al. 3D-Printed Hydrogel-Filled Microneedle Arrays. *Adv. Health Mater.* **2021**, *10*, 2001922. [CrossRef]

271. Yeung, C.; Chen, S.; King, B.; Lin, H.; King, K.; Akhtar, F.; Diaz, G.; Wang, B.; Zhu, J.; Sun, W.; et al. A 3D-printed microfluidic-enabled hollow microneedle architecture for transdermal drug delivery. *Biomicrofluidics* **2019**, *13*, 064125. [CrossRef]

272. Uddin, J.; Scoutaris, N.; Economidou, S.N.; Giraud, C.; Chowdhry, B.Z.; Donnelly, R.F.; Douroumis, D. 3D printed microneedles for anticancer therapy of skin tumours. *Mater. Sci. Eng. C* **2020**, *107*, 110248. [CrossRef]

273. Economidou, S.N.; Pere, C.P.P.; Reid, A.; Uddin, J.; Windmill, J.F.; Lamprou, D.A.; Douroumis, D. 3D printed microneedle patches using stereolithography (SLA) for intradermal insulin delivery. *Mater. Sci. Eng. C* **2019**, *102*, 743–755. [CrossRef]

274. Krieger, K.J.; Bertollo, N.; Dangol, M.; Sheridan, J.T.; Lowery, M.M.; O'cearbhaill, E.D. Simple and customizable method for fabrication of high-aspect ratio microneedle molds using low-cost 3D printing. *Microsyst. Nanoeng.* **2019**, *5*, 42. [CrossRef] [PubMed]

275. Farias, C.; Lyman, R.; Hemingway, C.; Chau, H.; Mahacek, A.; Bouzos, E.; Mobed-Miremadi, M. Three-Dimensional (3D) Printed Microneedles for Microencapsulated Cell Extrusion. *Bioengineering* **2018**, *5*, 59. [CrossRef]

276. Xenikakis, I.; Tzimtzimis, M.; Tsongas, K.; Andreadis, D.; Demiri, E.; Tzetzis, D.; Fatouros, D.G. Fabrication and finite element analysis of stereolithographic 3D printed microneedles for transdermal delivery of model dyes across human skin in vitro. *Eur. J. Pharm. Sci.* **2019**, *137*, 104976. [CrossRef] [PubMed]

277. Gittard, S.D.; Miller, P.R.; Jin, C.; Martin, T.N.; Boehm, R.D.; Chisholm, B.J.; Stafslien, S.J.; Daniels, J.W.; Cilz, N.; Monteiro-Riviere, N.A.; et al. Deposition of antimicrobial coatings on microstereolithography-fabricated microneedles. *JOM* **2011**, *63*, 59–68. [CrossRef]

278. Lu, Y.; Mantha, S.N.; Crowder, D.C.; Chinchilla, S.; Shah, K.N.; Yun, Y.H.; Wicker, R.B.; Choi, J.-W. Microstereolithography and characterization of poly(propylene fumarate)-based drug-loaded microneedle arrays. *Biofabrication* **2015**, *7*, 045001. [CrossRef]

279. El-Sayed, N.; Vaut, L.; Schneider, M. Customized fast-separable microneedles prepared with the aid of 3D printing for nanoparticle delivery. *Eur. J. Pharm. Biopharm.* **2020**, *154*, 166–174. [CrossRef] [PubMed]

280. Lim, S.H.; Tiew, W.J.; Zhang, J.; Ho, P.C.-L.; Kachouie, N.N.; Kang, L. Geometrical optimisation of a personalised microneedle eye patch for transdermal delivery of anti-wrinkle small peptide. *Biofabrication* **2020**, *12*, 035003. [CrossRef]

281. Johnson, A.R.; Caudill, C.L.; Tumbleston, J.R.; Bloomquist, C.J.; Moga, K.A.; Ermoshkin, A.; Shirvanyants, D.; Mecham, S.J.; Luft, J.C.; DeSimone, J.M. Single-Step Fabrication of Computationally Designed Microneedles by Continuous Liquid Interface Production. *PLoS ONE* **2016**, *11*, e0162518. [CrossRef] [PubMed]

282. Caudill, C.; Perry, J.L.; Iliadis, K.; Tessema, A.T.; Lee, B.J.; Mecham, B.S.; Tian, S.; DeSimone, J.M. Transdermal vaccination via 3D-printed microneedles induces potent humoral and cellular immunity. *Proc. Natl. Acad. Sci. USA* **2021**, *118*, e2102595118. [CrossRef] [PubMed]

283. Gittard, S.D.; Ovsianikov, A.; Chichkov, B.N.; Doraiswamy, A.; Narayan, R.J. Two-photon polymerization of microneedles for transdermal drug delivery. *Expert Opin. Drug Deliv.* **2010**, *7*, 513–533. [CrossRef] [PubMed]

284. Trautmann, A.; Roth, G.-L.; Nujiqi, B.; Walther, T.; Hellmann, R. Towards a versatile point-of-care system combining femtosecond laser generated microfluidic channels and direct laser written microneedle arrays. *Microsyst. Nanoeng.* **2019**, *5*, 6. [CrossRef] [PubMed]

285. Aksit, A.; Arteaga, D.N.; Arriaga, M.; Wang, X.; Watanabe, H.; Kasza, K.E.; Lalwani, A.K.; Kysar, J.W. In-vitro perforation of the round window membrane via direct 3-D printed microneedles. *Biomed. Microdevices* **2018**, *20*, 47. [CrossRef] [PubMed]

286. Wu, L.; Park, J.; Kamaki, Y.; Kim, B. Optimization of the fused deposition modeling-based fabrication process for polylactic acid microneedles. *Microsyst. Nanoeng.* **2021**, *7*, 58. [CrossRef] [PubMed]

287. Antonara, L.; Dallas, P.P.; Rekkas, D.M. A novel 3D printing enabled method for fast and reliable construction of polymeric microneedles using experimental design. *J. Drug Deliv. Sci. Technol.* **2022**, *68*, 102888. [CrossRef]

288. Loh, J.M.; Lim, Y.J.L.; Tay, J.T.; Cheng, H.M.; Tey, H.L.; Liang, K. Design and fabrication of customizable microneedles enabled by 3D printing for biomedical applications. *Bioact. Mater.* **2024**, *32*, 222–241. [CrossRef] [PubMed]

289. Uddin, J.; Scoutaris, N.; Klepetsanis, P.; Chowdhry, B.; Prausnitz, M.R.; Douroumis, D. Inkjet printing of transdermal microneedles for the delivery of anticancer agents. *Int. J. Pharm.* **2015**, *494*, 593–602. [CrossRef]

290. Ngo, T.D.; Kashani, A.; Imbalzano, G.; Nguyen, K.T.Q.; Hui, D. Additive Manufacturing (3D Printing): A Review of Materials, Methods, Applications and Challenges. *Compos. Part B Eng.* **2018**, *143*, 172–196. [CrossRef]

291. Yadav, V.; Sharma, P.K.; Murty, U.S.; Mohan, N.H.; Thomas, R.; Dwivedy, S.K.; Banerjee, S. 3D printed hollow microneedles array using stereolithography for efficient transdermal delivery of rifampicin. *Int. J. Pharm.* **2021**, *605*, 120815. [CrossRef] [PubMed]

292. Choo, S.; Jin, S.; Jung, J. Fabricating High-Resolution and High-Dimensional Microneedle Mold through the Resolution Improvement of Stereolithography 3D Printing. *Pharmaceutics* **2022**, *14*, 766. [CrossRef] [PubMed]

293. Vinayakumar, K.B.; Silva, M.D.; Martins, A.; Mundy, S.; González-Losada, P.; Sillankorva, S. Levofloxacin-Loaded Microneedles Produced Using 3D-Printed Molds for *Klebsiella Pneumoniae* Biofilm Control. *Adv. Ther.* **2023**, *6*, 2200320. [CrossRef]

294. Yang, Q.; Zhong, W.; Liu, Y.; Hou, R.; Wu, Y.; Yan, Q.; Yang, G. 3D-printed morphology-customized microneedles: Understanding the correlation between their morphologies and the received qualities. *Int. J. Pharm.* **2023**, *638*, 122873. [CrossRef]

295. Turner, J.G.; Laabei, M.; Li, S.; Estrela, P.; Leese, H.S. Antimicrobial releasing hydrogel forming microneedles. *Mater. Sci. Eng. C* **2023**, *151*, 213467. [CrossRef]

296. Yao, W.; Li, D.; Zhao, Y.; Zhan, Z.; Jin, G.; Liang, H.; Yang, R. 3D Printed Multi-Functional Hydrogel Microneedles Based on High-Precision Digital Light Processing. *Micromachines* **2020**, *11*, 17. [CrossRef]

297. Mathew, E.; Pitzanti, G.; dos Santos, A.L.G.; Lamprou, D.A. Optimization of Printing Parameters for Digital Light Processing 3D Printing of Hollow Microneedle Arrays. *Pharmaceutics* **2021**, *13*, 1837. [CrossRef]

298. Shin, D.; Hyun, J. Silk fibroin microneedles fabricated by digital light processing 3D printing. *J. Ind. Eng. Chem.* **2021**, *95*, 126–133. [CrossRef]

299. Sachan, R.; Nguyen, A.K.; Lu, J.; Erdmann, D.; Zhang, J.Y.; Narayan, R.J. Digital light processing-based 3D printing of polyte-trafluoroethylene solid microneedle arrays. *MRS Commun.* **2021**, *11*, 896–901. [CrossRef]

300. Wu, X.; Sun, Q.; Qiao, W.; Cui, J.; Chen, L. Rapid fabrication of customizable microneedle molds using digital light processing 3D printing methods. In Proceedings of the First Optics Frontier Conference, Hangzhou, China, 18 June 2021; p. 118500N. [CrossRef]

301. Monou, P.K.; Andriotis, E.G.; Tsongas, K.; Tzimtzimis, E.K.; Katsamenis, O.L.; Tzetzis, D.; Anastasiadou, P.; Ritzoulis, C.; Vizirianakis, I.S.; Andreadis, D.; et al. Fabrication of 3D Printed Hollow Microneedles by Digital Light Processing for the Buccal Delivery of Actives. *ACS Biomater. Sci. Eng.* **2023**, *9*, 5072–5083. [CrossRef]

302. Erkus, H.; Bedir, T.; Kaya, E.; Tinaz, G.B.; Gunduz, O.; Chifiriuc, M.-C.; Ustundag, C.B. Innovative transdermal drug delivery system based on amoxicillin-loaded gelatin methacryloyl microneedles obtained by 3D printing. *Materialia* **2023**, *27*, 101700. [CrossRef]

303. Lee, B.J.; Hsiao, K.; Lipkowitz, G.; Samuelsen, T.; Tate, L.; DeSimone, J.M. Characterization of a 30 μm pixel size CLIP-based 3D printer and its enhancement through dynamic printing optimization. *Addit. Manuf.* **2022**, *55*, 102800. [CrossRef]

304. Rajesh, N.U.; Coates, I.; Driskill, M.M.; Dulay, M.T.; Hsiao, K.; Ilyin, D.; Jacobson, G.B.; Kwak, J.W.; Lawrence, M.; Perry, J.; et al. 3D-Printed Microarray Patches for Transdermal Applications. *JACS Au* **2022**, *2*, 2426–2445. [CrossRef] [PubMed]

305. Doraiswamy, A.; Jin, C.; Narayan, R.; Mageswaran, P.; Mente, P.; Modi, R.; Auyeung, R.; Chrisey, D.; Ovsianikov, A.; Chichkov, B. Two photon induced polymerization of organic–inorganic hybrid biomaterials for microstructured medical devices. *Acta Biomater.* **2006**, *2*, 267–275. [CrossRef] [PubMed]

306. Rad, Z.F.; Prewett, P.D.; Davies, G.J. Rapid prototyping and customizable microneedle design: Ultra-sharp microneedle fabrication using two-photon polymerization and low-cost micromolding techniques. *Manuf. Lett.* **2021**, *30*, 39–43. [CrossRef]

307. Pillai, M.M.; Ajesh, S.; Tayalia, P. Two-photon polymerization based reusable master template to fabricate polymer microneedles for drug delivery. *MethodsX* **2023**, *10*, 102025. [CrossRef] [PubMed]

308. Fakeih, E.; Aguirre-Pablo, A.A.; Thoroddsen, S.T.; Salama, K.N. Fabrication and Characterization of Porous Microneedles for Enhanced Fluid Injection and Suction: A Two-Photon Polymerization Approach. *Adv. Eng. Mater.* **2023**, *25*, 2300161. [CrossRef]

309. He, Z.; Chen, F.; He, S. Fabrication of microneedles using two photon-polymerization with low numerical aperture. *Opt. Commun.* **2024**, *553*, 130093. [CrossRef]

310. Economidou, S.N.; Uddin, J.; Marques, M.J.; Douroumis, D.; Sow, W.T.; Li, H.; Reid, A.; Windmill, J.F.; Podoleanu, A. A novel 3D printed hollow microneedle microelectromechanical system for controlled, personalized transdermal drug delivery. *Addit. Manuf.* **2021**, *38*, 101815. [CrossRef]

311. Rodgers, A.M.; McCrudden, M.T.C.; Vincente-Perez, E.M.; Dubois, A.V.; Ingram, R.J.; Larrañeta, E.; Kissenpfennig, A.; Donnelly, R.F. Design and characterisation of a dissolving microneedle patch for intradermal vaccination with heat-inactivated bacteria: A proof of concept study. *Int. J. Pharm.* **2018**, *549*, 87–95. [CrossRef]

312. Boopathy, A.V.; Mandal, A.; Kulp, D.W.; Menis, S.; Bennett, N.R.; Watkins, H.C.; Wang, W.; Martin, J.T.; Thai, N.T.; He, Y.; et al. Enhancing humoral immunity via sustained-release implantable microneedle patch vaccination. *Proc. Natl. Acad. Sci. USA* **2019**, *116*, 16473–16478. [CrossRef] [PubMed]

313. Park, J.; Kim, Y.-C. Topical delivery of 5-fluorouracil-loaded carboxymethyl chitosan nanoparticles using microneedles for keloid treatment. *Drug Deliv. Transl. Res.* **2020**, *11*, 205–213. [CrossRef] [PubMed]

314. Zhang, T.; Sun, B.; Guo, J.; Wang, M.; Cui, H.; Mao, H.; Wang, B.; Yan, F. Active pharmaceutical ingredient poly(ionic liquid)-based microneedles for the treatment of skin acne infection. *Acta Biomater.* **2021**, *115*, 136–147. [CrossRef] [PubMed]

315. Ning, X.; Wiraja, C.; Chew, W.T.S.; Fan, C.; Xu, C. Transdermal delivery of Chinese herbal medicine extract using dissolvable microneedles for hypertrophic scar treatment. *Acta Pharm. Sin. B* **2021**, *11*, 2937–2944. [CrossRef] [PubMed]

316. Chen, Z.; Hu, X.; Lin, Z.; Mao, H.; Qiu, Z.; Xiang, K.; Ke, T.; Li, L.; Lu, L.; Xiao, L. Layered GelMA/PEGDA Hydrogel Microneedle Patch as an Intradermal Delivery System for Hypertrophic Scar Treatment. *ACS Appl. Mater. Interfaces* **2023**, *15*, 43309–43320. [CrossRef] [PubMed]

317. Meng, S.; Wei, Q.; Chen, S.; Liu, X.; Cui, S.; Huang, Q.; Chu, Z.; Ma, K.; Zhang, W.; Hu, W.; et al. MiR-141-3p-Functionalized Exosomes Loaded in Dissolvable Microneedle Arrays for Hypertrophic Scar Treatment. *Small* **2023**, *20*, e2305374. [CrossRef]

318. Huang, Y.; Li, J.; Wang, Y.; Chen, D.; Huang, J.; Dai, W.; Peng, P.; Guo, L.; Lei, Y. Intradermal delivery of an angiotensin II receptor blocker using a personalized microneedle patch for treatment of hypertrophic scars. *Biomater. Sci.* **2023**, *11*, 583–595. [CrossRef] [PubMed]

319. Zhao, W.; Zheng, L.; Yang, J.; Li, Y.; Zhang, Y.; Ma, T.; Wang, Q. Dissolving microneedle patches-mediated percutaneous delivery of tetramethylpyrazine for rheumatoid arthritis treatment. *Eur. J. Pharm. Sci.* **2023**, *184*, 106409. [CrossRef]

320. Ding, H.; Cui, Y.; Yang, J.; Li, Y.; Zhang, H.; Ju, S.; Ren, X.; Ding, C.; Zhao, J. ROS-responsive microneedles loaded with integrin avβ6-blocking antibodies for the treatment of pulmonary fibrosis. *J. Control. Release* **2023**, *360*, 365–375. [CrossRef]

321. Ben David, N.; Richtman, Y.; Gross, A.; Ibrahim, R.; Nyska, A.; Ramot, Y.; Mizrahi, B. Design and Evaluation of Dissolvable Microneedles for Treating Atopic Dermatitis. *Pharmaceutics* **2023**, *15*, 1109. [CrossRef]

322. Ye, G.; Jimo, R.; Lu, Y.; Kong, Z.; Axi, Y.; Huang, S.; Xiong, Y.; Zhang, L.; Chen, G.; Xiao, Y.; et al. Multifunctional natural microneedles based methacrylated Bletilla striata polysaccharide for repairing chronic wounds with bacterial infections. *Int. J. Biol. Macromol.* **2024**, *254*, 127914. [CrossRef] [PubMed]

323. Long, L.-Y.; Liu, W.; Li, L.; Hu, C.; He, S.; Lu, L.; Wang, J.; Yang, L.; Wang, Y.-B. Dissolving microneedle-encapsulated drug-loaded nanoparticles and recombinant humanized collagen type III for the treatment of chronic wound via anti-inflammation and enhanced cell proliferation and angiogenesis. *Nanoscale* **2022**, *14*, 1285–1295. [CrossRef] [PubMed]

324. Cai, Y.; Xu, X.; Wu, M.; Liu, J.; Feng, J.; Zhang, J. Multifunctional zwitterionic microneedle dressings for accelerated healing of chronic infected wounds in diabetic rat models. *Biomater. Sci.* **2023**, *11*, 2750–2758. [CrossRef] [PubMed]

325. Lu, M.; Zhang, X.; Xu, D.; Li, N.; Zhao, Y. Encoded Structural Color Microneedle Patches for Multiple Screening of Wound Small Molecules. *Adv. Mater.* **2023**, *35*, e2211330. [CrossRef]

326. Samant, P.P.; Niedzwiecki, M.M.; Raviele, N.; Tran, V.; Mena-Lapaix, J.; Walker, D.I.; Felner, E.I.; Jones, D.P.; Miller, G.W.; Prausnitz, M.R. Sampling interstitial fluid from human skin using a microneedle patch. *Sci. Transl. Med.* **2020**, *12*, eaaw0285. [CrossRef] [PubMed]

327. Xiao, J.; Zhang, S.; Liu, Q.; Xu, T.; Zhang, X. Microfluidic-based plasmonic microneedle biosensor for uric acid ultrasensitive monitoring. *Sens. Actuators B Chem.* **2024**, *398*, 134685. [CrossRef]

328. Zheng, L.; Zhu, D.; Xiao, Y.; Zheng, X.; Chen, P. Microneedle coupled epidermal sensor for multiplexed electrochemical detection of kidney disease biomarkers. *Biosens. Bioelectron.* **2023**, *237*, 115506. [CrossRef]

329. He, Q.-Y.; Zhao, J.-H.; Du, S.-M.; Li, D.-G.; Luo, Z.-W.; You, X.-Q.; Liu, J. Reverse iontophoresis generated by porous microneedles produces an electroosmotic flow for glucose determination. *Talanta* **2024**, *267*, 125156. [CrossRef]

330. Huang, H.; Qu, M.; Zhou, Y.; Cao, W.; Huang, X.; Sun, J.; Sun, W.; Zhou, X.; Xu, M.; Jiang, X. A microneedle patch for breast cancer screening via minimally invasive interstitial fluid sampling. *Chem. Eng. J.* **2023**, *472*, 145036. [CrossRef]

331. Park, W.; Maeng, S.-W.; Mok, J.W.; Choi, M.; Cha, H.J.; Joo, C.-K.; Hahn, S.K. Hydrogel Microneedles Extracting Exosomes for Early Detection of Colorectal Cancer. *Biomacromolecules* **2023**, *24*, 1445–1452. [CrossRef]

332. Abd-El-Azim, H.; Tekko, I.A.; Ali, A.; Ramadan, A.; Nafee, N.; Khalafallah, N.; Rahman, T.; Mcdaid, W.; Aly, R.G.; Vora, L.K.; et al. Hollow microneedle assisted intradermal delivery of hypericin lipid nanocapsules with light enabled photodynamic therapy against skin cancer. *J. Control. Release* **2022**, *348*, 849–869. [CrossRef] [PubMed]

333. Ma, Y.; Liu, Y.; Wang, Y.; Gao, P. Transdermal codelivery system of resveratrol nanocrystals and fluorouracil@ HP-β-CD by dissolving microneedles for cutaneous melanoma treatment. *J. Drug Deliv. Sci. Technol.* **2024**, *91*, 105257. [CrossRef]

334. Xu, R.; Guo, H.; Chen, X.; Xu, J.; Gong, Y.; Cao, P.; Wei, C.; Xiao, F.; Wu, D.; Chen, W.; et al. Smart hydrothermally responsive microneedle for topical tumor treatment. *J. Control. Release* **2023**, *358*, 566–578. [CrossRef]